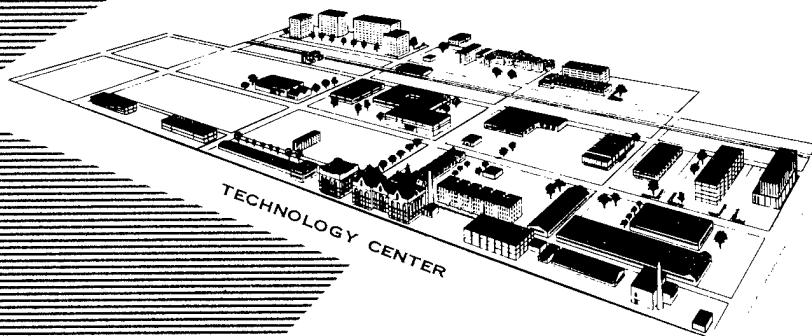ARF

ARF 4132-12

ARMOUR RESEARCH FOUNDATION OF ILLINOIS INSTITUTE OF TECHNOLOGY

TECHNOLOGY CENTER

1, Blast, physical water (pressure) & steam).

2. Pressure Waves in Water-Steam mixtures

PROPAGATION OF PRESSURE WAVES IN

A MIXTURE OF WATER AND STEAM

H. B. Karplus

AEC Research and Development Report
Contract No. AT(11-1)-528

DISTRIBUTION STATEMENT A
Approved for Public Release
Distribution Unlimited

20011105 066

LEGAL NOTICE

ARMOUR RESEARCH FOUNDATION
of
ILLINOIS INSTITUTE OF TECHNOLOGY
Technology Center
Chicago 16, Illinois

PROPAGATION OF PRESSURE WAVES IN

A MIXTURE OF WATER AND STEAM

H. B. Karplus

January 1961

This is the final technical report on a study of pressure wave propagation in liquids containing gas or vapor bubbles, such as the coolant fluid of boiling-water nuclear power reactors, performed by Armour Research Foundation for the United States Atomic Energy Commission. This work was initiated under Argonne National Laboratory Subcontract No. W31-109-eng-38-882, ARF No. A114, and was subsequently completed under U.S. Atomic Energy Commission Contract No. AT(11-1)-528 as Task No. 8, ARF No. D132A13. The work reported herein was performed from January 1958 through August 1960.

Computations and experiments have been recorded in Foundation logbooks No. C-7648, C-7708, C-7853, C-7926, C-8304, C-8818, and C-8955. Foundation personnel who have contributed materially to this work include M. D. Burkhard, H. B. Karplus, and L. A. Schmidt.

Respectfully submitted,

ARMOUR RESEARCH FOUNDATION OF
ILLINOIS INSTITUTE OF TECHNOLOGY

H. B. Karplus, Task Engineer

R. R. Whymark, Supervisor
Acoustics Research

APPROVED:

L. Reiffel, Director
Physics Research

Report No.
ARF 4132-12

ABSTRACT

The velocity of sound in mixtures of water and steam has been computed from the slope of the lines of equal entropy over a wide range of ambient conditions up to the critical point. The sound velocity is lower in the mixture than in either constituent. It changes discontinuously on transition to the single phase in wet steam with just a trace of liquid. The velocity is about 10 per cent less than in dry steam. The velocity decreases monotonically with increasing water content. In boiling water the velocity is very low. The smallest value occurs at reduced pressure at the triple point (with no solid ice present); the velocity here is as low as 0.012 m/s.

Rankine-Hugoniot curves were calculated for the mixture. These show that a shock-like compression in very wet steam or boiling water will condense all the steam, giving rise to a large change in volume with very little rise in pressure. The Hugoniot curve lies very close to a line of constant entropy in this case. For high quality steam the compression will raise the temperature of the vapor and evaporate the liquid phase. This occurs far from constant entropy conditions, indicating a strong loss mechanism.

In boiling water the propagation was studied with pressure waves having an amplitude exceeding the minimum necessary to condense all the steam. The velocity decreases monotonically with decreasing driving pressure, approaching the small amplitude acoustic velocity when the driving pressure approaches the minimum necessary to condense all the steam.

In a straight pipe of boiling water true shocks were not propagated. The rise time of the compression wave steadily increases as it passes

Report No.
ARF 4132-12

through the medium. On finally reaching a region of no bubbles, high peak pressures are observed. These peaks were an order of magnitude greater than the original driving pressure. This amplitude is apparently due to the formation of a water hammer.

TABLE OF CONTENTS

TABLE OF CONTENTS (CONT'D)

LIST OF ILLUSTRATIONS

Report No.
ARF 4132-12

LIST OF TABLES

Report No.
ARF 4132-12

LIST OF SYMBOLS

Symbol		Definition
A_o, B_o, A_1, B_1	=	constants in pressure-volume relation
c	=	sound velocity
E	=	specific internal energy
G	=	constant related to system of units
H	=	quantity of heat
J	=	mechanical equivalent of heat
L	=	latent heat of vaporization, fluid column length
p	=	absolute pressure
P	=	water hammer pressure amplitude
q	=	steam quality
s	=	fluid column length
S	=	specific entropy
t	=	time
T	=	absolute temperature, surface tension
u, v	=	particle velocity
V	=	specific volume
W	=	compression work
α	=	volume concentration of steam
γ	=	ratio of specific heats
ρ	=	density

Subscript

o:	refers to equilibrium thermodynamic reference state
1, 2:	refer to equilibrium thermodynamic states

LIST OF SYMBOLS (CONT'D)

Subscript

e: refers to change of parameter on evaporation

f: refers to liquid fraction of mixture

g: refers to vapor fraction of mixture

Other incidental notation is defined where it appears in the text.

PROPAGATION OF PRESSURE WAVES

IN A MIXTURE OF WATER AND STEAM

I. INTRODUCTION

The acoustic properties of reactor media are of interest in the determination of the propagation of shocks generated by a malfunction. The design of enclosures must be based on precise knowledge of the forces generated, and the acoustic impedance and attenuation of the medium.

The problem of a liquid-gas mixture was treated in a previous report[1] giving calculations and measurements of the velocity of sound in a water-air mixture. The propagation of shocks through such a mixture has been studied in England[2]. This present report is concerned with single component two phase liquid-vapor mixtures, specifically water-steam mixtures, in which the total mass of either phase will change with the changing pressure of a passing acoustic wave. The behavior therefore differs from liquid-gas systems, velocity of propagation being exceedingly low in the boiling fluid.

II. COMPUTATION OF PRESSURE PROPAGATION

IN A WATER-STEAM MIXTURE

In a two phase medium such as steam and water, the propagation constants of a pressure wave depend on the thermodynamic variables of the two states: latent heat, specific heat and density. A wave passing through a water-air mixture, for example, has a velocity determined by the average compressibility and density of the constituents. As a result, the medium behaves like a fluid having a high density like water and a high compressibility

---

[1]Superscript numerals refer to bibliography section.

like air. The pressure wave compresses the air because of its relatively lower stiffness, but not the water. Also, the compression is practically isothermal because of the enormous heat capacity of the water. If the gas is a vapor intermixed with its liquid phase at equilibrium, pressure is uniquely related to temperature so that if equilibrium is maintained, a change in pressure produces a change in temperature and relative mass and volume of each phase through condensation and evaporation. Sound waves of small pressure amplitude propagate through the vapor-liquid medium isentropically. Intermediate amplitude and shock waves propagate nonisentropically with dissipation of appreciable amounts of energy. The following discussion begins with small amplitude wave propagation in an intermixed vapor-liquid medium, in which account is taken of the change of state which occurs during the pressure cycle.

A.   Small Amplitude Sound Waves

1.   Propagation Velocity

The velocity of small amplitude sound waves in liquid-vapor mixtures is derived on the assumption of instantaneous equilibrium conditions at all points in the system. If the mixing of the two components is intimate enough, equilibrium will rapidly be attained. Put another way, for any given particle size of each phase there will exist a time in which equilibrium will be established. Frequency much smaller than the reciprocal of this time will be propagated under equilibrium conditions. We are concerned here with this low-frequency approximation. The value of this limit is discussed in Appendix H.

In a liquid-vapor equilibrium system, pressure and temperature are uniquely related. For each value of pressure there exists one and only one value of temperature, so that a rise in pressure is accompanied by a rise in temperature. This change in conditions causes some evaporation or condensation to take place producing a relatively large change in volume.

Now if we take into account the volume change due to the change in pressure of the vapor, and the change in mass of vapor due to evaporation or condensation, a total rate of change of volume (or its reciprocal: density) with pressure may be derived. In Appendix A we have derived this rate of change of pressure, p, with density, ρ, at constant entropy, S, analytically. This rate of change is equal to the square of the velocity of sound, c:

$$c^2 = (\partial p / \partial \rho)_S . \tag{1}$$

In terms of specific volume of fluid, V_f ; specific entropy of fluid, S_f ; the changes of these quantities upon evaporation, V_e and S_e ; and the quality, q (relative mass of steam), the velocity is given by

$$c = (q\, V_e + V_f) \left[q\, \frac{V_e}{S_e}\, \frac{dS_e}{dp} - q\, \frac{dV_e}{dp} + \frac{V_e}{S_e}\, \frac{dS_f}{dp} - \frac{dV_f}{dp} \right]^{-1/2} . \tag{2}$$

Let us look at pressure-density curves, Fig. 1, and see how the slopes of these lines change with given conditions. We observe that the lines, though of necessity continuous through the liquid-mixture and mixture-vapor transitions, do not have continuous slopes; the lines actually kink sharply, having a lower slope in the mixture than in either phase. This slope (if plotted on linear instead of logarithmic paper) is

equal to the square of the sound velocity. It is seen that the slopes are greatest in pure water on the right and least in the mixture immediately adjacent to it, that is, in boiling water containing a small quantity of steam. The very low velocity of sound in boiling water with low steam content may be understood by realizing that a very small pressure change condenses a large fraction of the available vapor to give a large percentage change in the over-all density. We are, of course, assuming an acoustic pressure that is so small that the vapor content will decrease without vanishing during the positive half cycles. Similar limiting considerations apply to the discontinuous velocity change when the vapor-fluid mixture approaches the pure vapor region. It is of interest to observe in Fig. 1 that a pressure increase in high quality steam (relative mass of steam large) brings the mixture closer to the pure vapor region. This is due to the adiabatic temperature rise which causes some of the liquid to evaporate. When the mass of liquid is large, this heat is absorbed and a pressure increase condenses some steam. The dividing line between evaporation and condensation for a water-steam mixture is close to the 50 per cent concentration at all ambient pressures. If water droplets in steam or vapor bubbles in liquid have exceedingly small radii (an assumption necessary to extend the range of the low-frequency approximation), then the effect of surface tension will become noticeable. In that case equilibrium conditions demand a difference in pressure across the curved interface. This differential has been neglected in the present treatment, limiting the low-frequency approximation.

The velocity of sound as given by Eq. (2) was computed for many values of pressure (or temperature) and quality. The values of specific

volume and entropy were taken from Keenan and Keyes: <u>Thermodynamic</u> <u>Properties of Steam</u> .[3] The derivatives were obtained by using a chord approximation, taking values from alternate lines in the steam tables. The errors introduced by this technique are quite small as shown in Appendix B. The variation of velocity with temperature and quality is shown in Fig. 2. A somewhat similar graph is shown as Fig. 3 with a change of variable for the abscissa which replaces temperature with the logarithm of the pressure. With this change of variable the sound velocity approximates a linear function of the independent variable, the logarithm of pressure, at very low steam concentrations. Individual curves correspond to specified values of the quality of steam, q. In Fig. 4 velocity has been plotted as a function of quality or phase concentration at selected values of pressure, p (or the corresponding values of temperature, T). A monotonic increase in velocity with concentration for all pressure is exhibited. The rate of increase of velocity with quality, q, is largest for a pressure in the region of 100 lb in.$^{-2}$ while it is smaller for pressures both below and above this value. As the critical point is approached, the energy required for a phase change vanishes, so that concentration becomes meaningless and the sound velocity-quality curve approaches a horizontal line. In Fig. 5 the same curves are plotted on a logarithmic scale. Here the variations at the lower concentrations are emphasized. We note that in water containing just a few steam bubbles, a very low sound velocity compared to the velocity in pure water is derived. The change to the high velocity in pure water is discontinuous.

The computations have been extended to the condition of pure dry steam, and the results are presented in graphical form in Fig. 6. It is observed that at the same temperature and pressure pure dry steam has a higher velocity than wet steam, even when the water content tends to zero; that is to say, we compute a discontinuous jump in the velocity at this point also. This is clearly shown in Fig. 6, in which velocity is plotted as a function of pressure for constant entropy. Lines of constant quality and lines of constant temperature are also shown. At low pressures and high temperatures, velocity is reasonably independent of pressure as one would expect for a perfect gas. At higher pressures and lower temperatures these lines tend to curve down. It is interesting to note here that if instead of plotting velocity as a function of temperature, we plot it as a function of constant enthalpy, as in Fig. 7, the velocity is almost independent of pressure, even up to very high pressures, provided condensation does not take place; see also Fig. 8. When condensation does take place we can observe discontinuous velocity changes when the slightest trace of condensation occurs. The region of very high pressures and low enthalpy, in which the lines are seen not to be perfectly horizontal, is rather uncertain because the points tabulated in the steam tables are too far apart for a determination of the differential parameters as required by Eq. (1). The difference between the water-steam mixture and water-air mixture, covered in our previous study[1], is brought out in Fig. 6, where we see that for constant entropy the velocity of sound rises very slightly with pressure at high entropy, more slowly in fact than in a single phase medium, and at low entropy or low quality, the velocity actually decreases with increasing pressure.

Report No.
ARF 4132-12

2. Comparison with Data from the Literature

There have been relatively few measurements of the velocity of sound in steam. Velocity was measured by a resonance technique by Masson[4] in 1857; Jaeger[5] in 1889 used a Kundt's tube technique; and Treitz[6] reported on the velocity of sound in steam in 1903. Comparison of the observations with our computation is summarized in Table I. It is seen that the results of Jaeger and of Treitz are at variance with those of Shilling[7] (1924) and those of Billhartz and Bishop[8] (1936). Shilling was very careful to remove liquid water droplets and also obtained his results at the end point or extrapolation of a series of measurements in superheated steam.

It is very tempting to assume that the steam used by Jaeger and by Treitz contained water droplets. For the measurements of saturated steam (at 100°C and below) an assumption of about 14 per cent by weight of water would bring these observations in line with computations. This, of course, does not explain Treitz' results at 110, 120, 130°C at atmospheric pressure.

To explain these we postulate that even in slightly superheated steam liquid droplets will exist. Surface tension provides an excess pressure inside the droplet so that it is in equilibrium with the vapor at the same temperature. This leads to a stable droplet of radius $r = 2 T/(p_b - p_a)$, where T is the surface tension and $(p_b - p_a)$ is the difference between ambient pressure and boiling pressure at that temperature. In the case of Treitz' work droplet radii of the order of 10^{-4} cm are calculated. These may well escape observation, being no larger than a wavelength of light.

Changes in diameter will of course have an effect on the equilibrium conditions because of the change in surface energy. The smaller the radius the larger the error introduced by neglecting this effect. For

droplets with radii greater than $2T/L\rho$ (T = surface tension, dyne cm^{-2}, L = latent heat, dyne cm gm^{-1}, ρ = density, gm cm^{-3}) the surface tension effect is smaller than the latent heat effect. Even for the droplets of 10^{-4} cm radii postulated above, surface tension has a negligible effect on the sound velocity and is justifiably neglected.

Evidence for the existence of liquid droplets in superheated vapor is found in the effectiveness of and necessity for the special filters Shilling used to remove droplets during his measurements, all of which were at atmospheric pressure and above 100°C. It is also worth noting that the above relation for the radius, $r = 2T/(p_b - p_a)$, yields zero radius above the critical temperature when the surface tension vanishes. This means that there are no droplets in "permanent" gases (i.e., gases above the critical temperature which cannot be liquefied by simple compression).

The formula also yields an infinite radius for droplets in saturated steam. Frenkel[10] postulates that droplets in saturated steam are hotter than the average temperature of the vapor and are surrounded by a thin layer of superheated vapor. As they lose heat by conduction, they grow in size and will eventually fall.

Droplets in superheated steam will remain the equilibrium size, larger ones evaporating and smaller ones gathering more condensation. Ultimately collision between droplets and between droplets and walls causes the larger agglomerate to evaporate down to the stable size, thus slowly eliminating the liquid phase.

Table 1

THE VELOCITY OF SOUND IN STEAM

Observer	Temp. °C	c reported m/s	c calculated wet* $q \to 0$	dry**
Masson[3]	0	402		
Jaeger[4]	93	402	434	469
Jaeger	96	410	437	472
Treitz[5]	100	404. 3	439	475
Treitz	110	413. 0	444	478
Treitz	120	417. 5	449	482
Treitz	130	424. 4	455	488
Shilling[6]	100	471. 5	439	473. 1
Shilling	300	593. 2	***	586
Shilling	600	727. 8	***	714
Shilling	800	795. 3	***	787
Billhartz and Bishop[7]	100	471. 3	439	473. 1

* According to Eq. (2).

** According to $c^2 = \gamma\, p\, V_g$; values of γ and V_g were taken from steam tables[3].

*** Liquid not stable at atmospheric pressure at this temperature.

B.   An Empirical Expression for the Pressure-Volume

Relation at Constant Entropy

An expression has been obtained which gives the specific volume V
of a water-steam mixture in terms of specific entropy, S, and pressure, p:

$$V = A_o (S + 0.24) p^{-1} + B_o (S - 0.76) p^{-0.7}. \tag{3}$$

Values of A_o and B_o are given for several systems of units in Table 2.
The expression is an approximate fit of the measured values of entropy and
pressure. Accuracy of the parameters A_o and B_o is better than 10 per
cent in the range $0.1 < p < 3200$ lb in.$^{-2}$ (ice point to critical point), and
is better than 4 per cent over the most important part of the range between
15 and 2500 lb in.$^{-2}$. However, when S is less than about 0.5, the value
for V is the small difference between large quantities, and the expression
is not reliable. Further work is needed to obtain a good expression for
small entropies.

A functional relation of this kind greatly facilitates differentiation to
obtain an approximate value for sound velocity, and integration under an
adiabatic line to obtain work done if no heat is lost. The form of the
function is relatively easy to handle.

The velocity of sound is

$$c = V (-\partial p / \partial V)_S^{1/2} ,$$

$$= V \left[A_o (S + 0.24) p^{-2} + 0.7 B_o (S - 0.76) p^{-1.7} \right]^{-1/2} . \tag{4}$$

The work done going from condition V_1 to V_2 at constant entropy is

$$W = \int_{V_1}^{V_2} p \, dV,$$

$$= \int_{P_1}^{P_2} p \left(\frac{\partial V}{\partial p}\right)_S dp,$$

$$= A_1(S+0.24) \log (p_1/p_2) + B_1(S-0.76)(p_1^{0.3} - p_2^{0.3}), \quad (5)$$

where $A_1 = A_o$ and $B_1 = 2.33 \, B_o$ in a consistent system of units. For other systems see Table 2.

The method of obtaining Equation (3), the expression for volume in terms of pressure, is detailed in Appendix D.

C.   Rankine-Hugoniot Curves for Pressures up to

Complete Condensation or Evaporation

The change of specific volume V and specific internal energy E across a shock front are given in terms of the pressure p by the well-known Rankine-Hugoniot relationship,

$$E_2 - E_1 = (1/2)(p_1 + p_2)(V_1 - V_2), \quad (6)$$

where the subscripts 1 and 2 refer to conditions before and after the shock.

Table 2

PARAMETERS FOR THE PRESSURE-VOLUME RELATION

$$V = A_o (S + 0.24) p^{-1} + B_o (S - 0.76) p^{-0.7}$$

Units of Parameters		Specific Energy				
p	V		A_o	B_o	A_1	B_1
lb in.$^{-2}$	ft^3 lb^{-1}	lb in.$^{-2}$ft^{3}lb^{-1}	113	67.5	A_o	157
lb in.$^{-2}$	ft^3 lb^{-1}	Btu lb^{-1}	113	67.5	610	847
dyne cm^{-2}	cm^{2}gm^{-1}	erg gm^{-1}	4.9×10^8	1.0×10^7	A_o	2.4×10^7
newton m^{-2}	m^3/kg	joule kgm^{-1}	4.9×10^4	2.0×10^3	A_o	4.8×10^3
atmospheres	cm^{3}gm^{-1}	cal gm^{-1}	480	640	2.0×10^4	6.0×10^4

Note: For the specific entropy S, 1 Btu/°F lb = 1 cal/°C gm;

hence S_o = 0.24 Btu/°F lb

= 0.24 cal/°C gm.

In the case of a water-steam mixture we get the additional four relationships

$$V_1 = q_1 V_{e1} + V_{f1} , \qquad V_2 = q_2 V_{e2} + V_{f2} ,$$

and

$$E_1 = q_1 E_{e1} + E_{f1} , \qquad E_2 = q_2 E_{e2} + E_{f2} ,$$

for conditions 1 and 2.

For an equilibrium process (that is, after completion of relaxations near the wave front) E_2 and q_2 are eliminated between these equations. We obtain then

$$V_2 = \frac{(p_1 + p_2) V_1 + 2G (E_1 - E_{f2} + E_{e2} V_{f2}/V_{e2})}{(p_1 + p_2) + 2G (E_{e2}/V_{e2})} , \tag{7}$$

where the constant G is unity for a consistent system of units. In our case where steam tables give p in lb in^{-2}, V in ft^3 lb^{-1}, and E in Btu lb^{-1} the factor G is 5.4046.

Two Rankine-Hugoniot curves are shown in Fig. 9, where V_2 has been plotted against p_2. For the first case, curve (a), p_1 has been chosen as 14.7 lb in.$^{-2}$ and V_1 as 1 ft^3 lb^{-1}. For the second, curve (b), p_1 is 14.7 lb in.$^{-2}$ and V_1 is 10 ft^3 lb^{-1}. We note that the quantity E_1 is determined once p_1 and V_1 have been specified, and that the quantities E_{e2}, V_{f2}, and V_{e2} are constants of the fluid-gas mixture. The curve constructed of short dashes gives the pairs of values for pressure and specific volume at constant entropy.

We observe that for curve (a), when a pressure of 29 lb in.$^{-2}$ or about 2 atmospheres is reached, all steam has been condensed to water and the volume has been reduced to 1/60th of its original value. This

would require a large amount of energy. We observe further that if we draw an adiabat through the final point, it almost exactly coincides with the Rankine-Hugoniot curve. A similar curve could be plotted starting with a specific volume of 0.1 ft^3/lb in which case the pressure reached for complete condensation does not exceed 16 lb in.$^{-2}$. That is, a sixfold volume reduction would be observed with less than a 10 per cent pressure increase. In general, in bubbly water (less than 50 per cent steam by volume) a very small pressure increase will condense all the steam. The energy required to do this (since pressure is essentially constant) is of course simply p V, where V is the total volume of steam. Thus any explosion with less than this amount of energy could never produce a significant pressure increase in an equilibrium process. The value of the minimum pressure needed to condense all the steam in a mixture is discussed in Section II-D-3 and in Appendix E.

If we were to consider, for example, an initial condition of 250 ft^3 of water-steam mixture containing 20 per cent steam by volume at a pressure of 700 lb in.$^{-2}$, the pressure increase required to condense all the steam adiabatically may be arrived at as follows:

volume of water	200 ft^3
volume of steam	50 ft^3
entropy	1.425 Btu/lb°F

Interpolation in the steam tables show that this entropy corresponds to water without steam at 725 lb in.$^{-2}$ pressure.

Thus in this case there is a pressure rise of about 3.5 per cent. To obtain the energy required to perform this compression it is a fair approximation to consider the work done in compressing this steam as $\overline{p}$ V, where

$\bar{p}$ is the average pressure, or 712 lb in.$^{-2}$.

$$W = 712 \times 50 \text{ lb in.}^{-2} \text{ ft}^3,$$

$$= 6590 \text{ Btu},$$

$$= 1.65 \times 10^6 \text{ cal.}$$

This shows that if the energy released in the mixture in this example is less than about 1.6 million calories, there will be very little eventual pressure build-up at the wall of the containing vessel. On the other hand, if the energy release is greatly in excess of this pressure amplification may occur, as shown in Section II-D.

The other case, illustrated in curve (b) of Fig. 9, starts with wet steam of specific volume 10 ft^3 lb^{-1} at one atmosphere of pressure. In this case the shock is seen to evaporate water until, at a pressure of about 680 lb in.$^{-2}$, pure steam remains. In this case the Rankine-Hugoniot curves and the adiabat are separated leaving the steam in a state of higher quality, at a higher pressure in a given volume, and with higher specific energy. Energy is obviously required to increase the energy in this manner and the only possible source is the shock wave itself. The energy of the shock must therefore be attenuated in traveling through the medium.

In order to compute the energy under the adiabat, Eq. (5) of Section II-B is useful. For $p_2 = 680$ lb in.$^{-2}$, $p_1 = 14.7$ lb in.$^{-2}$, $S = 1.433$,

$$W = 610 (1.433 + 0.24) \log_e \frac{680}{14.7} +$$

$$847 (1.433 - 0.76) (680^{0.3} - 14.7^{0.3}),$$

$$= 6673 \text{ Btu/lb.}$$

D.   Propagation of Large Amplitude Pressure Waves

1.   General Description of Events

The preceding section described the behavior of shocks of small amplitude, so that the mixed medium remained a mixture after the event. In boiling liquid in which the original density is within 25 per cent of that of the liquid the pressure required to condense all the steam was shown to be very small (Fig. 9; see also Appendix E). We now consider larger pressures which condense all the steam to a single liquid state. These were also studied experimentally (see Section III).

The application of a pressure pulse to the boiling liquid causes the steam bubbles near the surface to collapse, and a wave of bubble collapse travels away from the point of application of the pressure until all the vapor is condensed. The events are shown schematically in Figs. 10, 11 and 12 for an arrangement in which a shock wave is applied from above to the boiling water. Figure 10A shows the appearance of the liquid-vapor mixture extending from the surface down to some point m before the pulse is applied.   The region below m is filled with pure liquid. Some time after a pulse has been applied (Fig. 10B) the mixture in the region e - j has been condensed to pure liquid, and the surface has been displaced from d to e. By the time the front has reached m, the end surface is at point h, below the original level at d. First, we consider the events which would be observed with a pressure transducer at position c in Fig. 10 just above the liquid surface. At a time $t_1 = L_{bc}/c_1$ after release of a pressure wave at b, an abrupt pressure increase will be observed (Fig. 11). Here c_1 is the velocity of the shock wave in the gas above the boiling water, and L_{bc} is the distance from b to c.

At time $t_2 = t_1 + L_{cd} (\frac{1}{c_1} + \frac{1}{c_2})$, a reflection from the surface produces another abrupt pressure increase. Velocities c_1 and c_2 for the incident and the reflected shock waves differ only slightly from the velocity of sound c_o if small amplitude shock waves are used. For greater ease of reading we write c for an average transport velocity, so that $t_2 = t_1 + 2 L_{cd}/c$. A small reflection from expansion around the fixtures at the pressure release point b is next observed at time $t_3 = t_2 + 2 L_{bc}/c$. While these events have been occurring, a rarefaction due to sudden release of pressure in region a has been traveling up the driving tube. This rarefaction undergoes a reflection at the upper end of the tube and appears at position c at time $t_4 = (2 L_{ab} + L_{bc})/c$. The pressure pulse which passed point c at time t_2 traveling upward is also reflected at the top, and is observed again at c at time $t_5 = t_2 + 2 L_{ab}/c$. This sequence then repeats itself with slightly reduced amplitude on each succeeding pass. Several cycles of the event are sketched in the top part of Fig. 12.

Pressure-time functions in the liquid at the points i, j, k, o in Fig. 10 are also shown in Fig. 11. At point i immediately below the surface the pressure rises to the full amplitude of the reflected shock wave observed above the surface. This is easily explained by the boundary conditions on pressure and particle velocity at the interface between air and the dense water medium. The time of transit through the liquid to succeeding positions down the tube is evident. The attenuation of the wave also shows up as a reduction of the wave front slope. Finally, at time $t_6 = t_i + L_{dm}/c_f$ the interface between liquid and mixture has arrived at point m, and this instant a large pressure pulse is observed everywhere in the liquid. The velocity of this pulse in the mixture is denoted by c_f;

t_i is about half way between t_1 and t_2. The maximum amplitude of this pulse is much larger near the bottom of the mixture column than it is at the surface.

The details of this pressure pulse are shown in Figs. 13 and 14. Assumed here are a column of mixture of length a supported by a column of pure liquid of length b, which in turn is terminated by a rigid wall. The two cases of Figs. 13 and 14 show the slightly different behavior observed for a greater than and less than b.

Just before the last few bubbles collapse, we essentially see a column of liquid of length a, having a velocity v, approaching a stationary column of length b. A very short time t after impact, the particles in the impact region will travel with an intermediate velocity. Conservation of momentum (or symmetry) considerations dictate that with reference to this transition region the incoming velocities must be equal, i.e., v/2. Thus a wave with particle velocity v/2 travels in both direction from the point of impact (Figs. 13A and 14A). The pressure increase in this region, as shown in Figs. 12B and 13B, is equal to $p/2 = v \rho_f c_f / 2$, ρ_f and c_f being density and sound velocity for the pure water without bubbles. (For proof of this statement see Section III-D-3 below.) For the case b less than a as in Fig. 13, the pulse is first reflected at the rigid wall, doubling the pressure as shown at D. This double step pulse continues to travel to the free surface, where each step is reflected as shown at E-F, G-H to return down as a double step pulse with negative particle velocity as at I and pressure reduced to zero. The slight decay of pressure and velocity after reflection at the rigid end takes into account the fact that the boundary is a plate having large rigidity

but a finite mass. The applied pressure consequently starts it moving, giving finite velocities at this end in E, G, and I. The pulse traveling down again would become a negative pressure pulse on reflection as shown dotted at K-P. However, the liquid cannot support a negative pressure, especially near its boiling point, and no negative pulse is observed.

If the length a of the moving column is less than that of the fixed column b then events differ in detail from those just described. As seen in Fig. 14, the pulse traveling up toward the free surface is reflected first and a complete pulse with a positive front and negative return to zero travels down toward the rigid boundary. There it is reflected and gives rise to a pressure doubling at this point for a brief period until the rear of the pulse has also been reflected (F, H, J). This pulse, after further reflection at the free surface, would give rise to a negative pressure. The consequence of this negative pulse will be discussed after the pressure-time diagrams have been considered.

The pressure-time diagrams, Fig. 15, are almost self explanatory. They were obtained by considering the pressure variation from diagram to diagram in Figs. 13 and 14. If the moving column is shorter than the fixed column, then two distinct pulses will be observed (D, E) except for a very small region (F, G) near the rigid bottom. The separation vanishes at a distance a, equal to the length of the incoming liquid column. Near the surface the reflected wave tends to cancel the original wave in part because of the relatively slow rise time of the pressure pulse; hence the small amplitude in Fig. 15D. In the region near the rigid bottom a double step (Fig. 15F) is observed, the length of the halfway plateau being proportional to the distance from the bottom, vanishing completely at the bottom (see Fig. 15G).

-19-

When the fixed column is longer than the incoming moving column, it is difficult to move out of the region of the double step (Fig. 15B) without moving into the region of low amplitude (Fig. 15C) near the surface. If the fixed column length b is short enough, two pulses will not resolve at all.

The negative pulse previously considered is not observed because the liquid starts to boil again and the pulse is transmitted as a large reduction in density and very small reduction in pressure. This "density" pulse travels through the water just like a pressure pulse and is reflected at the surfaces. The velocity, however, is governed by water-steam mixture properties, so that the pressure remains at ambient until the positive reflection of the pulse in the free surface has traveled all the way down to the rigid bottom and there, on collapsing the last bubble, once again gives rise to a large pressure as before. A whole series of large amplitude pulses are thus observed with long intervals of constant ambient pressure. The intervals get progressively shorter as the amplitude of the pulse is attenuated. This is due to the fact that the negative pulse produces a smaller density reduction at each reflection. Experimental evidence is given in Section III-C, Figs. 23, 24.

2. Propagation Velocity of the Compression Wave

To calculate the velocity u with which the interface between the original mixture and the condensed liquid above it advances into the mixture, we use the conservation of mass and momentum across this pressure front. Observation has shown this interface to be a rather ill-defined region which continues to broaden as it progresses through the pipe. However, as far as points outside the region are concerned the

conservation laws hold. There is, of course, the difficulty of defining the velocity of the interface because of its finite, increasing thickness. However, the velocity u_f of the condensed fluid behind it is a perfectly well-defined velocity at any instant, if we consider a point sufficiently far removed from the interface so that this velocity is constant. Now the velocity of advance of an ideal interface is precisely related to the velocity of the water behind; we shall now compute these two velocities.

We define a velocity $u_2 = u_1 - u_f$ as the relative velocity of the interface with respect to the condensed fluid behind it; then the two conservation laws become, in terms of the densities ρ_1, ρ_2 and the pressures p_1, p_2 on the two sides of the interface

$$\rho_1 u_1 = \rho_2 u_2 , \qquad \text{(conservation of mass)} \qquad (8a)$$

$$\rho_1 u_1^2 - \rho_2 u_2^2 = p_2 - p_1 . \quad \text{(conservation of momentum)} \quad (8b)$$

For convenience we now define a steam volume concentration, α, as the volume of steam per unit volume of mixture. It is related to the mass concentration, q, used earlier by

$$(1 - 1/\alpha) = (1 - 1/q) \, V_f / V_g = (1 - 1/q) \, \rho_g / \rho_f .$$

The density of the mixture ρ_1 is:

$$\rho_1 = \alpha \rho_g + (1 - \alpha) \rho_f \cong (1 - \alpha) \rho_f \quad \text{if } \alpha < 0.9 , \qquad (9)$$

since at atmospheric pressure $\rho_f \cong 1600 \rho_g$. Thus

$$\rho_2 = \rho_f \cong \rho_1 / (1 - \alpha) . \qquad (10)$$

Substituting Eqs. (9), (10), into Eq. (8),

$$u_1{}^2 = (p_2 - p_1) \,/\, \alpha (1-\alpha) \rho_f \,. \tag{11a}$$

By using (8a), we get u_2 and $u_f = u_1 - u_2$:

$$u_2{}^2 = (p_2 - p_1)(1-\alpha) \,/\, \alpha \rho_f \,, \tag{11b}$$

$$u_f{}^2 = (p_2 - p_1) \alpha \,/\, (1-\alpha) \rho_f \,. \tag{11c}$$

It is of interest that the expression for the velocity u_1 has the same form as the velocity of sound in a water-air mixture[8], except that the ambient pressure p is now replaced with the driving pressure $(p_2 - p_1)$.

Some caution must be exercised in the use of the formula for velocity, since the derivation assumed complete condensation. There exists a pressure differential below which complete condensation does not take place. In Appendix E this minimum pressure is shown to be

$$(p_2 - p_1)_{min} = \alpha(1-\alpha)^{-1} V_f S_e V_g{}^{-1} (dS_f / dp)^{-1} \,. \tag{12}$$

For $\alpha = 0.5$ at $100°C$ ($212°F$), $(p_2 - p_1)_{min} = 0.18$ psi.
The value of $(p_2 - p_1)_{min}$ is plotted in Fig. 16.

It is also shown in Appendix E that when the pressure differential only barely condenses all the water, i.e., when $p_2 - p_1 = (p_2 - p_1)_{min}$, the velocity $(u_1)_{min}$ is very nearly equal to the small amplitude sound wave speed discussed in the first part of this report. Therefore we see that above this minimum driving pressure, propagation velocity decreases with the decreasing driving pressure until this driving pressure is so small that not all the steam is condensed. When this happens a further reduction of driving pressure has little effect on the propagation velocity.

3. **Pressure Buildup in a Water Hammer**

Consider two columns of water approaching each other with relative velocity u_f in an evacuated pipe. Since both columns are alike the velocity of the first particles to touch after collision will be the mean of the velocities of the two columns, i.e., $u_f/2$. This will be their velocity with respect to each column. Each column therefore sees a pressure wave advancing from the point of collision with a particle velocity $u_f/2$. If this wave travels along the column with velocity c, a length of column $\Delta L = c \Delta t$ will have stopped after the time Δt. This length has a mass $\rho A c \Delta t$. The change of momentum is $\rho A c \Delta t (u_f - 1/2 u_f)$, and the time rate of change of momentum becomes $\rho A c u_f/2$. This is equal to the total force $F = PA$. Hence the peak pressure $P = \rho c u_f/2$.

We may further introduce the concept of pressure amplification $P/(p_2 - p_1)$, when a driving pressure $p_2 - p_1$ produces in the fluid a velocity u_f which at the end of the bubble region produces the water hammer pulse P.

Thus

$$P = \rho_f c_f u_f/2 = (1/2) \rho_f c_f \sqrt{(p_2 - p_1)\alpha/(1 - \alpha)\rho_f}, \qquad (13)$$

And the pressure amplification becomes

$$P/(p_2 - p_1) = (1/2) c_f \left[\rho_f \alpha/(1 - \alpha)(p_2 - p_1) \right]^{1/2} \qquad (14)$$

$$= 75 \sqrt{\alpha/\left[(1 - \alpha)(p_{b2} - p_{b1})\right]}$$

$$= 287 \sqrt{\alpha/\left[(1 - \alpha)(p_{p2} - p_{p1})\right]},$$

where p_b is the pressure measured in bars and p_p is the pressure measured in psi.

4. Energy Loss

Consider a collapsing bubble. The radial velocity of the water surrounding it endows this shell of water with kinetic energy. When the bubble radius finally becomes zero, the radial velocity and the kinetic energy associated with it vanish. This energy is converted to heat. To calculate the energy dissipated in this manner we calculate the kinetic energy of the mass of water behind the "shock" front in our case and compare it with the work done on it by the force accelerating it.

Now from the velocity u_f and mass M, we may compute the kinetic energy of the slug, and from the applied pressure difference $(p_2 - p_1)$ and the distance s_g traveled, the work done (Fig. 17).

We use the symbol s_m to define the length of the mixture column, s_f the length of the final water column, and s_g the distance the upper surface has moved. Then

$$s_g = s_m - s_f \, ,$$

and

$$s_g = \alpha\, s_m \quad \text{and} \quad s_f = (1 - \alpha)\, s_g \, / \, \alpha.$$

The work W_1 done in compression by the driving air on the water column is

$$W_1 = (p_2 - p_1)\, As_g;$$

and the kinetic energy W_2 of the column is

$$W_2 = (1/2)\, \rho_f\, As_f\, (u_f)^2$$

$$= A\, s_f\, (p_2 - p_1)\, \alpha / 2\, (1 - \alpha),$$

where substitution was made from Eq. (11c). Therefore E, the mechanical energy lost per unit volume of vapor condensed, is

$$E = (W_1 - W_2) / A s_g = (p_2 - p_1) \left[1 - \alpha \, s_f / s_g \, 2 (1 - \alpha) \right] \tag{15}$$

$$= (p_2 - p_1) / 2.$$

Thus one half of the applied energy is lost in collapsing the bubbles and heating the water.

Of course, the water is heated also by the condensing steam giving up its latent heat. (This heating accounts for the minimum pressure required to collapse the bubbles.) A comparison of this heating effect with the energy loss of compression is instructive.

The heat H_s given up by condensing steam per unit volume is

$$H_s = L \, \rho_g \, ,$$

where L is the latent heat of steam and ρ_g its density. The heat H_e produced by the energy loss mechanism is

$$H_e = EJ,$$

where J is the mechanical equivalent of heat.

The heating effect due to the energy loss is thus a fraction $J (p_2 - p_1) / 2 \rho_g L$ of the heat produced by the condensing steam. In the vicinity of 100°C it would be necessary to have a pressure jump $(p_2 - p_1)$ of about 14 atmospheres or 200 psi before the two effects become equal. The amplitudes in the investigation were confined to fractions of an atmosphere, $(p_2 - p_1)$ about 10 psi; therefore no attempt was made to detect these very small energy losses by measuring water temperature changes. The heating due to the energy loss mechanism would be the small difference between the total heating and that of the latent heat liberation above. Initial

conditions were not controlled with the precision that would be required for a direct determination of the loss mechanism from the difference between these two relatively large quantities.

III. EXPERIMENTAL INVESTIGATION

A. Apparatus

The propagation of "shocks" of sufficient amplitude to condense all the vapor in a boiling water mixture was investigated with a transparent shock tube. The general components of the equipment are shown diagrammatically on Fig. 18 and pictorially on Fig. 19. The prominent feature is a Pyrex "double tough" glass pipe, which is the shock tube proper. It was necessary to employ a glass pipe because visual observation was needed to check on uniformity of bubble formation. The pressure gages were mounted on annular brass inserts between glass sections. In the illustration, gage holders are shown separated by 6 in. of glass pipe. Many readings were taken with a single insert having a gage separation of only 2 in. Narrow tubes are shown leading to a manometer which was used to determine the bubble concentration in the fluid. The void concentration is directly proportional to the height difference in the manometer limbs. The difference in density between the manometer fluid and the water in the pipe due to the temperature difference was easily corrected by calibration with a partially filled pipe.

Bubbles were produced by boiling the water with a wire heater. In the reflux arrangement shown a regular immersion heater boiled the water near the base. A separately adjustable heater in the region of the pressure gages helped to maintain a reasonably uniform bubble concentration. The steam formed was condensed in a water-cooled condenser

and the condensate was fed back to the system near the base.

The upper end of the pipe was joined to the driver section. This was a steel pipe of the same diameter as the main shock tube and separated from it by a thin diaphragm. In operation, the driver section was filled with compressed air and the diaphragm was burst and the shock wave impinged on the surface of the boiling water.

The pressure-time history in the boiling water was recorded with pressure gages on a cathode ray oscilloscope. The traces of two gages were plotted simultaneously through the use of an electronic switch (Tektronix 53/54C). The oscilloscope time base was started with a third transducer incorporated in the apparatus very close to the diaphragm. This assured the starting of the trace well in advance of the occurrence of events in the liquid. Oscilloscope traces were recorded photographically. Details of the pressure measurement and the diaphragm are given in Appendices F and G.

B.   Photography

The events of steam bubble compression as indicated by the oscilloscope traces occurred faster than the eye could follow. It seemed of interest to verify the sequence of events by means of high-speed photography. Three sets of pictures of these sequences are shown in Fig. 20. The time scale shown below in the first group applies to all three. Differences in film velocities have been accommodated by suitably mounting the prints. Water in the column boiled at atmospheric pressure. A shock wave of 12 psi was applied for the upper two sequences, and 22 psi for the lower one. We can see very clearly on these films that as the pressure wave travels down the pipe, steam bubbles slowly collapse. However, the bubble

Report No.
ARF 4132-12

collapse is by no means instantaneous, but bubbles are seen to contract and move down while others further down have already started to collapse. In fact, a small number of fairly large bubbles can be seen to complete their collapse long after those farther down have been completely cleared.

The pressure front is difficult to identify on the films, just as it was difficult to define on the oscilloscope traces; definition is lost continuously as the wave progresses. The velocity of the water itself is quite evident, however, from the bubble displacement in successive frames. These pictures confirm the analytical discussions presented earlier in the report.

C.   Experimental Results

On the basis of the motion of the liquid-vapor mixture under the influence of an incident shock wave, a sequence of pressure events has been described in Section II-D. These events were experimentally observed, including the low propagation velocity and the pressure amplification by water hammer action.

The velocity of propagation of the pulses was obtained from the time difference of the arrival of the pulse at the two pressure gages. It has been pointed out already that, in spite of the rapidly rising front of the shock wave striking the medium, the pressure rises slowly in the mixture. Moreover, the rate of rise decreases as the pulse progresses through the fluid. This is brought out in the upper oscillogram of Fig. 21.

The pressure is seen to rise at the lower gage (lower trace) about 0.8 ms after the start of the pulse at the upper gage, whereas the upper level or "knee" of the pulse is not reached until 2.2 ms after it was reached at the upper gage. This part of the trace is seen to approach

Report No.
ARF 4132-12

merging with the water-hammer pulse at 3.7 ms. Complete merging

is sometimes observed, as in the lower pair of oscillogram traces

of Fig. 4. This picture was taken with similar initial bubble concen-

tration, about 5 per cent, but with more amplifier gain as shown on

the ordinate scale.

The "shock" velocity is defined as the distance between the gages

divided by the time it takes the front to move from one to the other.

Because different parts of the front do not have the same travel time,

the concept of wave velocity is not a precise one. However because of

the very small value of this velocity, even an order-of-magnitude value

is of interest. Different velocities are of course obtained if we measure

the velocity of the start of the front or the velocity of the upper "knee".

These different velocities have been plotted in Fig. 22. The velocity of

the start is shown as a circle, the velocity of the "knee" as a triangle

and the midway points as squares. The diagram in upper corner of

the graphs shows the pressure-time function of the two gages; the time

interval indicated by the appropriate symbol divided into the gage

separation yields the velocity plotted on this graph by the corresponding

symbol.

The measured velocity of about 50 m/s (150 ft/s) at 5 per cent,

faling to 20 m/s (60 ft/s) at 50 per cent steam concentration is seen to

be somewhat higher than the computed velocity from Eq. (11a) as shown

in the solid line.

Experimental difficulty was predominantly connected with the

production of a uniform mixture, and measuring the bubble concentration

at the instant of breaking the diaphragm. It is seen that the very low

velocity predicted is confirmed, even though it was found difficult to obtain a high degree of precision in the measurements.

The rate of rise of pressure decreases as the pulse travels through the medium. The rate of rise is, moreover, usually rather irregular, which precludes precise statement about rate of the rise and its change. On the average it was found that, when the mixture was struck by a true shock on the surface, then at a depth of about 1 in. (2.5 cm) the pressure took about one half millisecond to rise to its final value; 2 in. (5 cm) further this rise time was nearly doubled.

The pressure pulse traveling through boiling water finally produces a large water hammer as described in Section II-D. This is seen as a tall spike at 3.7 ms on Fig. 21A. The amplitude of this final pulse was at first found to be not quite as large as predicted. A few measurements were attempted subsequently with a longer column of boiling water. Concentration uniformity was poorer. Fairly large concentrations were used and averaged over the length of the column by observing the increase in height of the column. Table 3 shows that the long column is needed to observe the full water hammer pulse. The need for the longer column is readily understood when we observe an expanded pulse, Fig. 23. The rise time for the pulse is consistently about 0.2 ms, so that when it is measured close to the initial surface, the reflection interferes destructively with the initial pulse. This is very readily seen when comparing the oscillograms in Figs. 23 and 24, where a much greater amplifier gain had to be used for the gage near the surface than for the one at the other end of the pipe. The correspondence of the upper trace of Fig. 23 with Fig. 15A, and the lower trace with Fig. 15C (inverted in Fig. 23 for convenience) confirms this behavior.

Report No.
ARF 4132-12

Table 3

PRESSURE AMPLIFICATION, $P/(p_2-p_1)$, FOR THE

WATER HAMMER

Concentration per cent	p_2-p_1 psi	$P/(p_2-p_1)$ measured	$P/(p_2-p_1)$ computed	Distance from Surface, in.
1	8	5	10	4
5	8	15	25	4
6	5	14	30	4
8	6	15	33	4
10	8	10	35	4
25	5	25	10	4
10	8	20	35	30
20	8	50	50	30
22	8	40	50	30
25	8	45	60	30

IV. CONSIDERATIONS OF FINITE BUBBLE COLLAPSE TIME

The experiments have led to valuable information regarding the formation of large amplitude pressure pulses which can be explained by the formation of a water hammer. The precision of experimental checks was limited by the difficulty of obtaining a uniform bubble mixture. The bubble concentration could be measured only as an average over the period of the manometer, whereas one really should know the instantaneous value at the time of the shock wave passage. This instantaneous bubble concentration as plotted in Fig. 22 is not known with desired precision. This accounts in part for the observed scatter of points about the predicted curve.

There appears to be a predominant scattering above the computed line. An explanation for this phenomenon was sought in the finite bubble collapse times which have been neglected in our derivation. The collapse of a single spherical cavity was studied by Rayleigh[9] using conservation of momentum. This was modified by Plesset and Zwick[12] to take into account heat transfer. Heat transfer was shown to have only a small effect on the collapsing bubble. This is in contrast with the bubble growing in a fluid superheated a few degrees, where the heat transfer slows up bubble growth by an order of magnitude compared with that predicted by momentum conservation[13,14].

Using Rayleigh's approximation for the time t_o required for a bubble of initial radius R_o to collapse completely,

$$t_o = 0.915 R_o \left[\rho_f / (P_2 - P_1) \right]^{1/2} .$$

Substituting in this the maximum pressure in our wave of 10 psi or 7×10^5

dyne cm^{-2}, a bubble of 0.5 cm radius will take about 700 microseconds to collapse. During the collapse of the bubble, some pressure is transmitted on through the fluid to the adjacent region while the bubble is collapsing. Consequently, the next region sees the pulse rising more slowly at first. The next region sees this initial rise further delayed and so on until the pulse takes a longer time to rise to its final value than it would take the bubble to collapse if this pressure were suddenly applied.

The bubbles in our 1.5 in. pipe were less than 1/2 in. in diameter, usually much less, so that a 0.5 cm radius bubble represents an upper limit. The rise time in our oscillograms is of the order of 1 to 2 milliseconds. The lack of bubble uniformity and consequent irregular pressure rise prohibit a precise measurement of this quantity. Considering the large order of magnitude by which the velocity measured here differs from typical velocities usually observed in single phase media, experiments and theory are in agreement. The water-hammer pulses had not been expected, though once they were observed, a very plausible explanation followed. The computation of the amplitude of these pulses yielded a pressure amplification factor which was confirmed by measurements in columns of adequate length. It must be conceded that the precision of these measurements was less than that of the earlier velocity measurements. Further work on the effect of bubble size would be desirable. The generation of bubbles of uniform and controlled size is necessary for the success of such experiments.

V.   CONCLUSIONS

Small amplitude sound waves propagate through fluid-vapor mixtures with very low velocities.   The velocity depends on the ambient condition of pressure (or temperature) and the relative quantity of the constituents. Further work along these lines is recommended.

Large amplitude waves in a mixture will completely eliminate one of the phases present.   If the initial liquid content is low, the liquid will be evaporated by the heat of compression, with the conversion of mechanical energy into heat.   For larger fluid fractions the heat is absorbed by the thermal capacity of the fluid and there is very little temperature or pressure rise in the mixture; the vapor condenses, converting the potential energy of the driving pressure partly into the kinetic energy of the condensed phase and partly into heat, when the inward velocity of the collapsing bubble surface vanishes on final collapse.   The kinetic energy of the moving condensed phase can give rise to very high amplitude pressure pulses upon encountering the boundary of the low impedance mixture.

On the other hand, an explosion of finite energy content can be completely absorbed in a mixture of sufficient volume.   Application of this phenomenon is discussed in Section II-C.   A system with spherical geometry as distinct from the linear geometry considered in this report merits further investigation.

Report No.
ARF 4132-12

BIBLIOGRAPHY

1. Karplus, H. B. Velocity of Sound in a Liquid Containing Gas Bubbles, Report No. COO-248, U.S. Atomic Energy Commission Contract No. AT(11-1)-528, Armour Research Foundation (June 1958)

2. Campbell, I. J., and A. S. Pitcher. Proc. Roy. Soc. 243, Ser. A., 1235, 535 (1958)

3. Keenan, J. H., and F. G. Keyes. Thermodynamic Properties of Steam, John Wiley and Sons, New York, N. Y. (1936)

4. Masson, A. Phil. Mag. 13, 533 (1857)

5. Jaeger, W. Annalen der Physik 36, 165 (1889)

6. Treitz, W. Bonn Dissertation (1903)

7. Shilling, W. H. Phil. Mag. 3, Ser. 7, 273 (1927)

8. Billhartz, W. H., and F. L. Bishop. J. Acoust. Soc. Am. 7, 225 (1936)

9. Rayleigh, Lord. Phil. Mag. 34, 94 (1917)

10. Frenkel, J. Kinetic Theory of Liquids, Ch. 7, Dover Publications (1955)

11. Landsberg, J., and C. R. Uhholmin, Bull. Ac. Sci. USSR 16, 399 (1937)

12. Zwick, S. A., and M. S. Plesset. J. Math. Phys. 33, 4, 308 (1955)

13. Plesset, M. S., and S. A. Zwick. J. App. Phys. 25, 474 (1956)

14. Forster, H. K, and N. Zuber. J. Appl. Phys. 25, 474 (1956)

15. Jakob, M., and G. A. Hawkins. Elements of Heat Transfer, John Wiley and Sons, New York, N. Y. (1958).
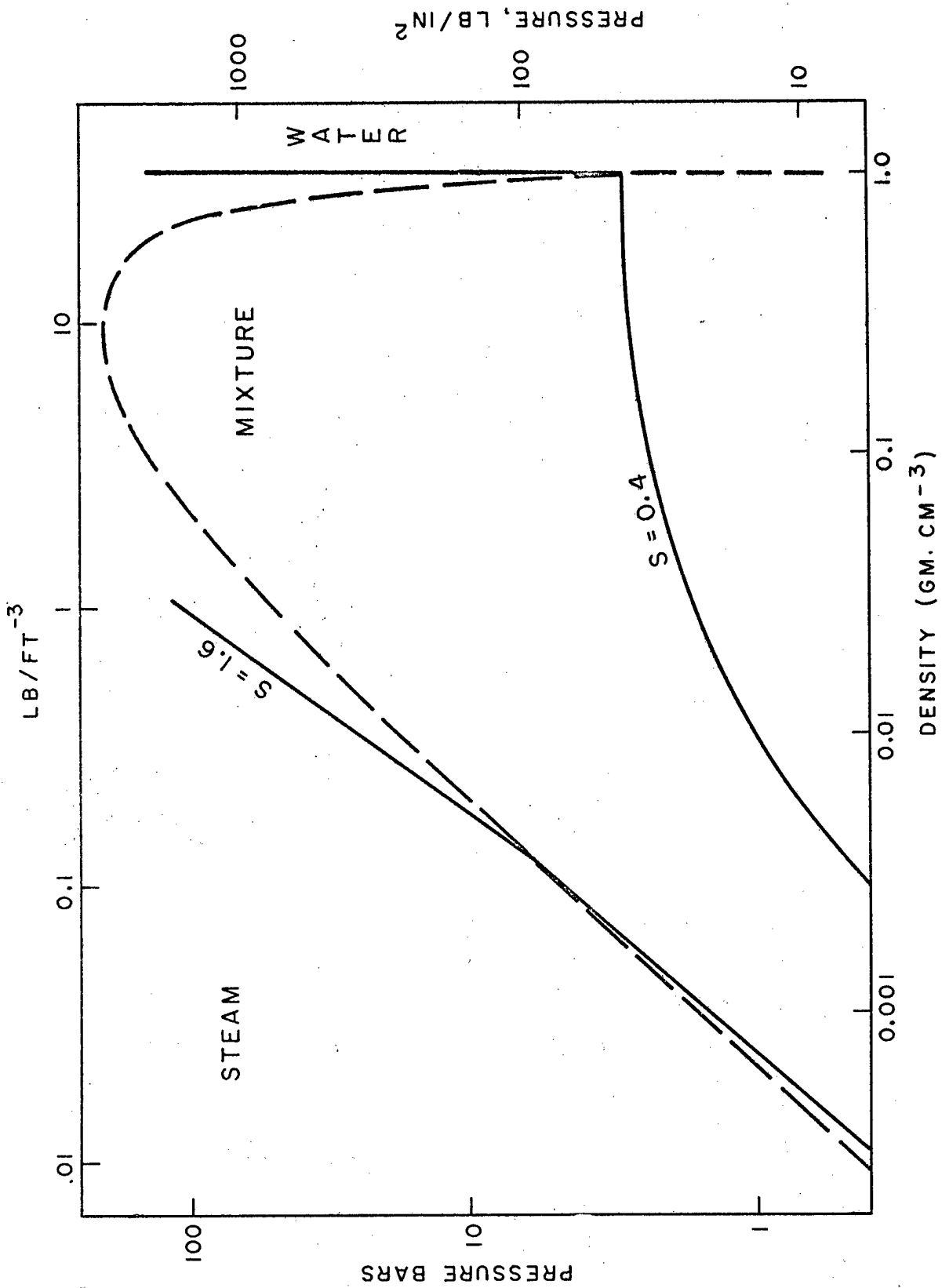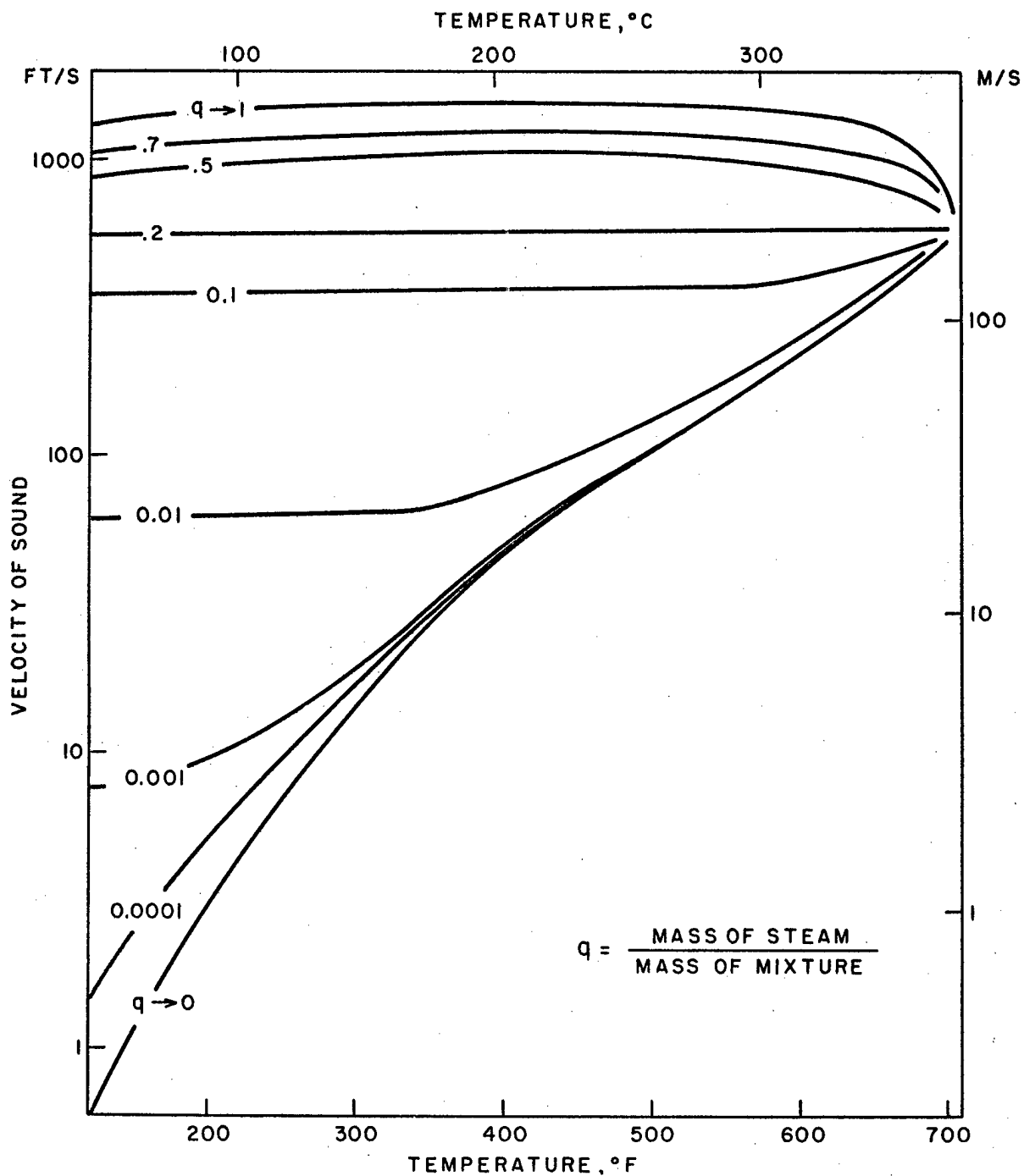
Fig. 1 LINES OF CONSTANT ENTROPY

Report No.
ARF 4132-12

Fig. 2   VELOCITY OF SOUND IN A WATER-STEAM MIXTURE
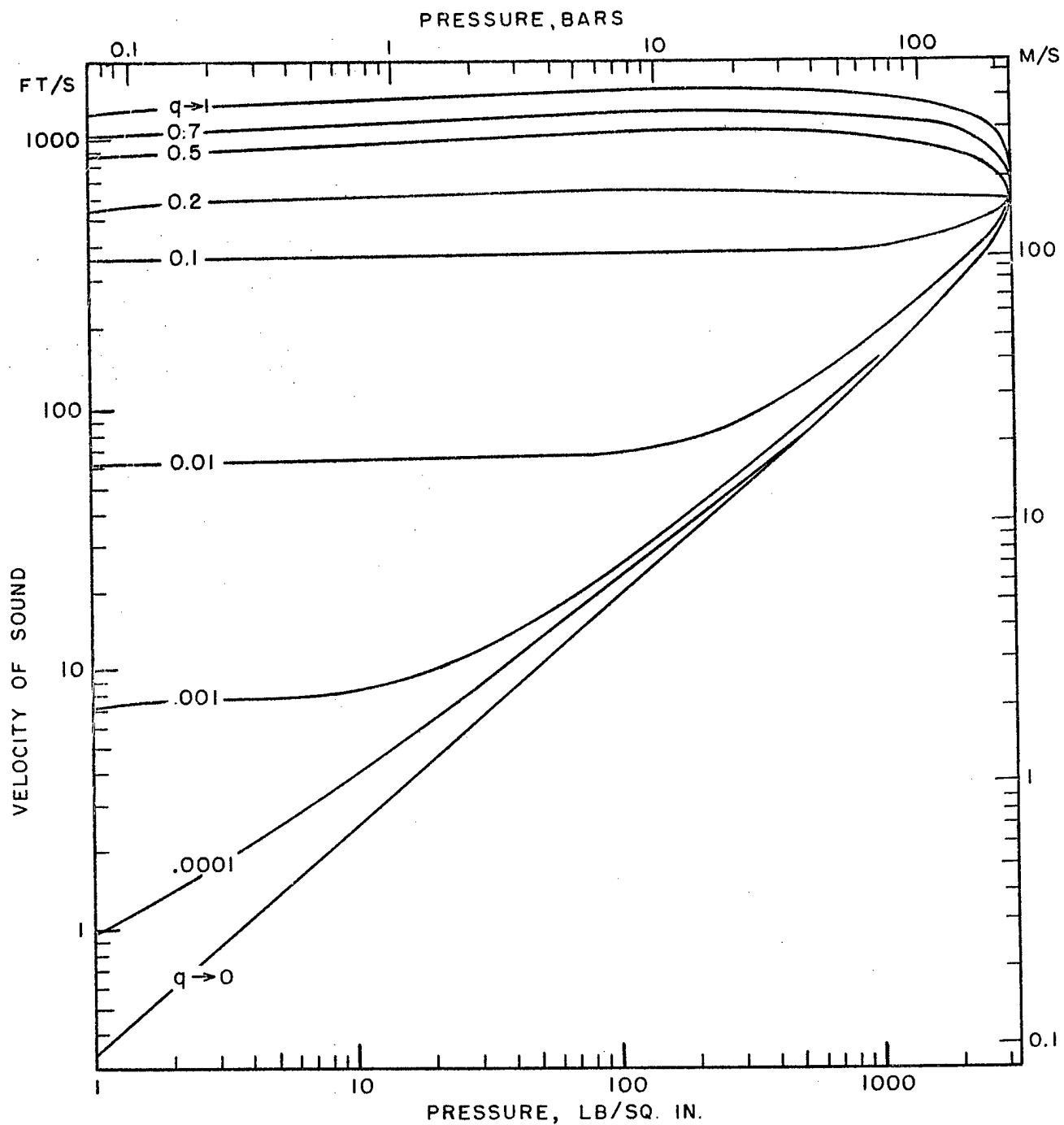
Fig. 3 VELOCITY OF SOUND IN STEAM AS A FUNCTION OF PRESSURE

FT/S

M/S

1600

1500

1400

1300

1200

1100

1000

900

800

700

600

500

400

300

200

100

0

VELOCITY OF SOUND

P, LB/IN^2

100

1000

10

T, °F

327

545

193

101

635

2000

400

300

695

3000

705 — — 3206 — —

200

2000

100

1000 LB/IN^2
545°F

1, 10

0   .1   .2   .3   .4   .5   .6   .7   .8   .9   1.0

$q = \dfrac{\text{MASS OF STEAM}}{\text{MASS OF MIXTURE}}$
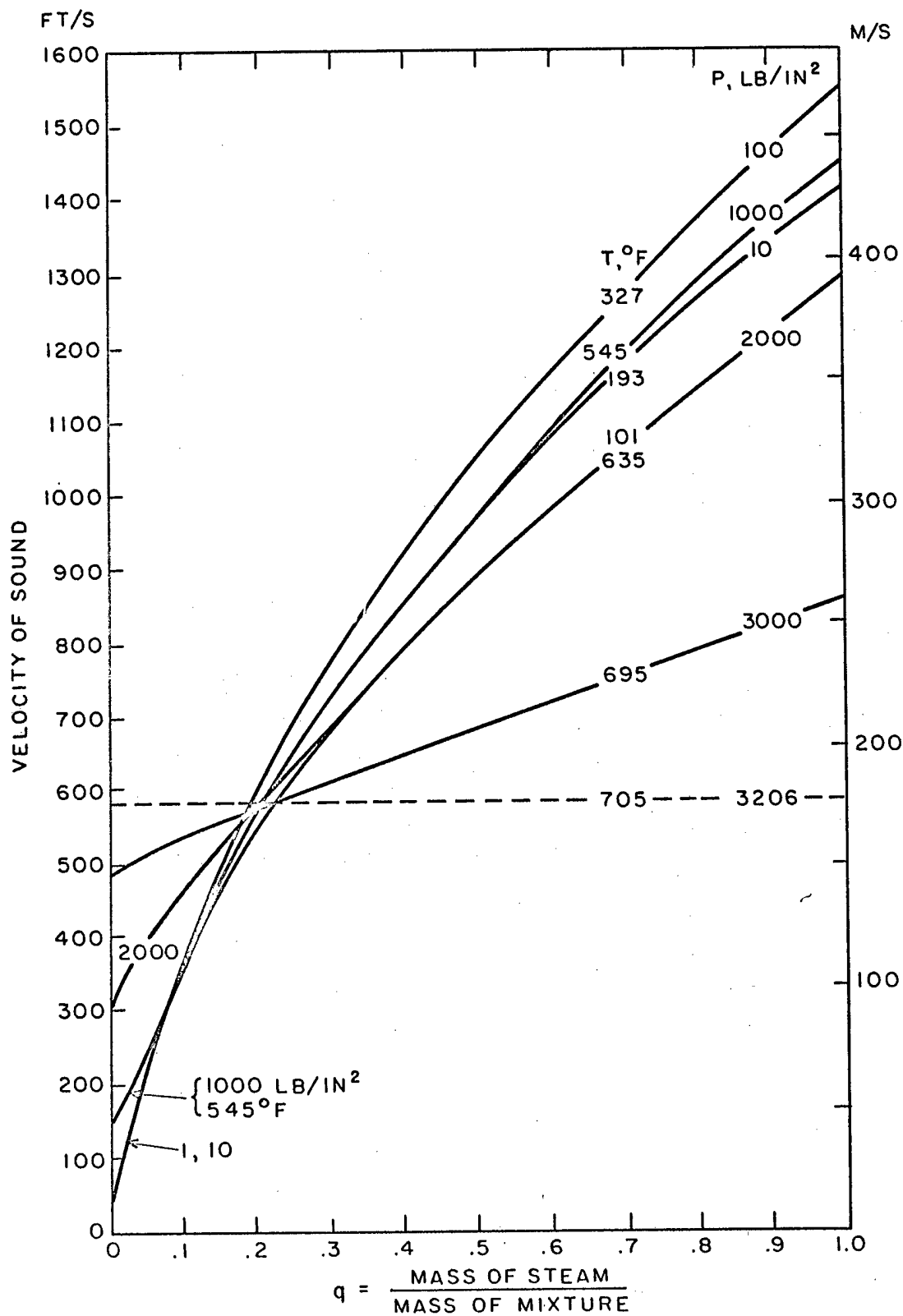
Fig. 4 VELOCITY OF SOUND AS A FUNCTION OF STEAM QUALITY
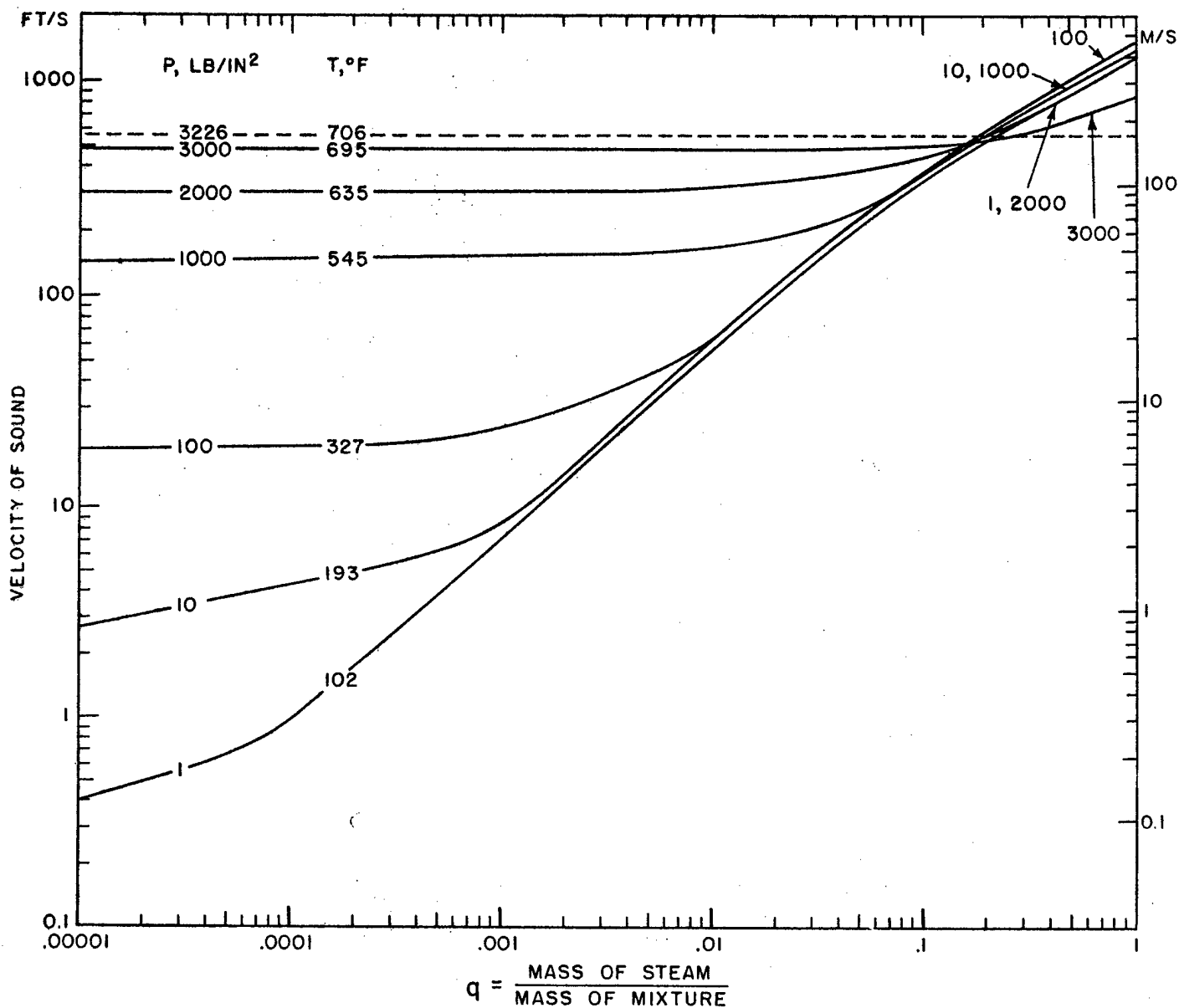
Fig. 5 VELOCITY OF SOUND AS A FUNCTION OF STEAM QUALITY
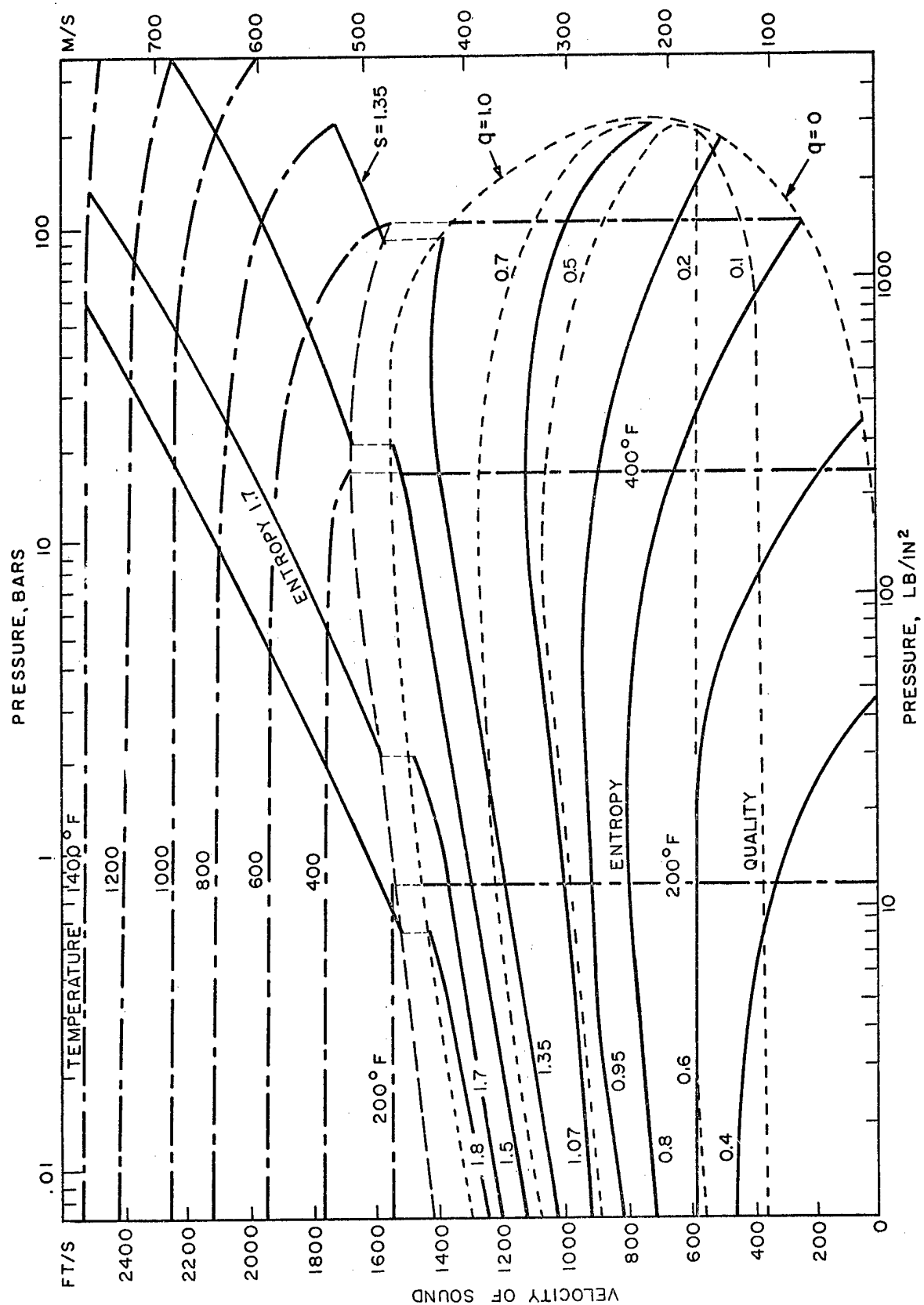
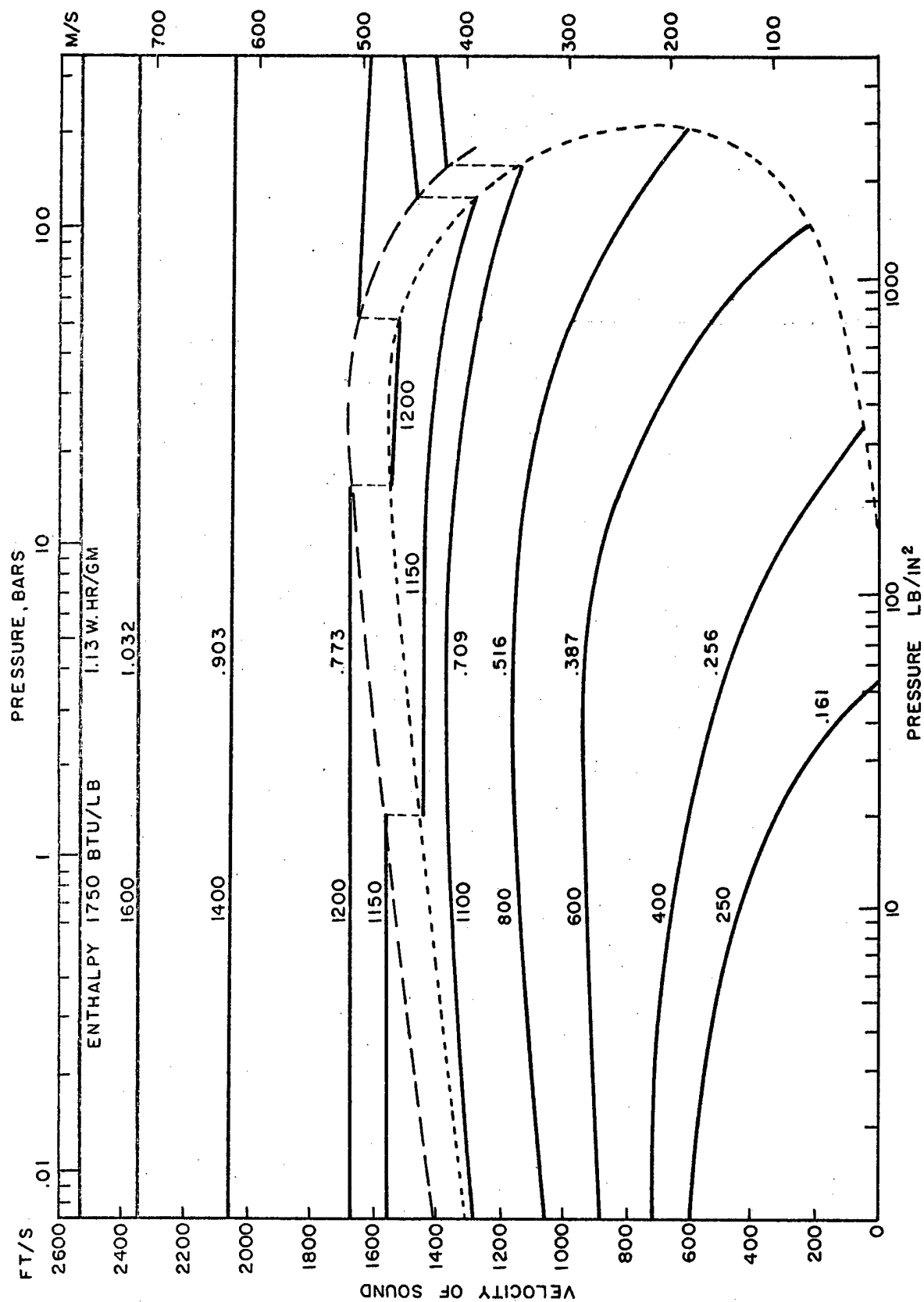Fig. 6 VELOCITY OF SOUND AS A FUNCTION OF PRESSURE
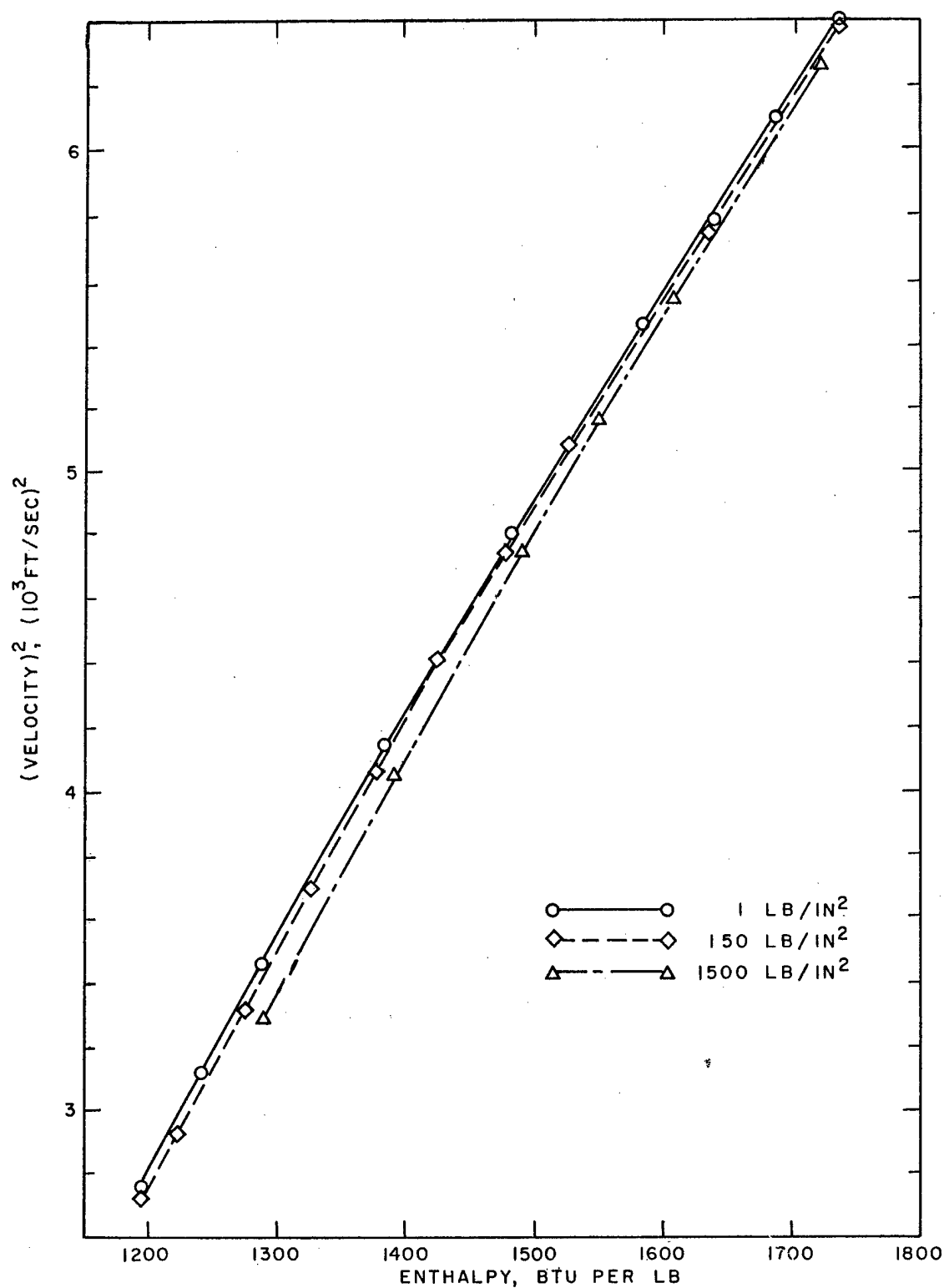
Fig. 7 VELOCITY OF SOUND AT CONSTANT ENTHALPY

-42-

Fig. 8 VELOCITY OF SOUND AS A FUNCTION OF
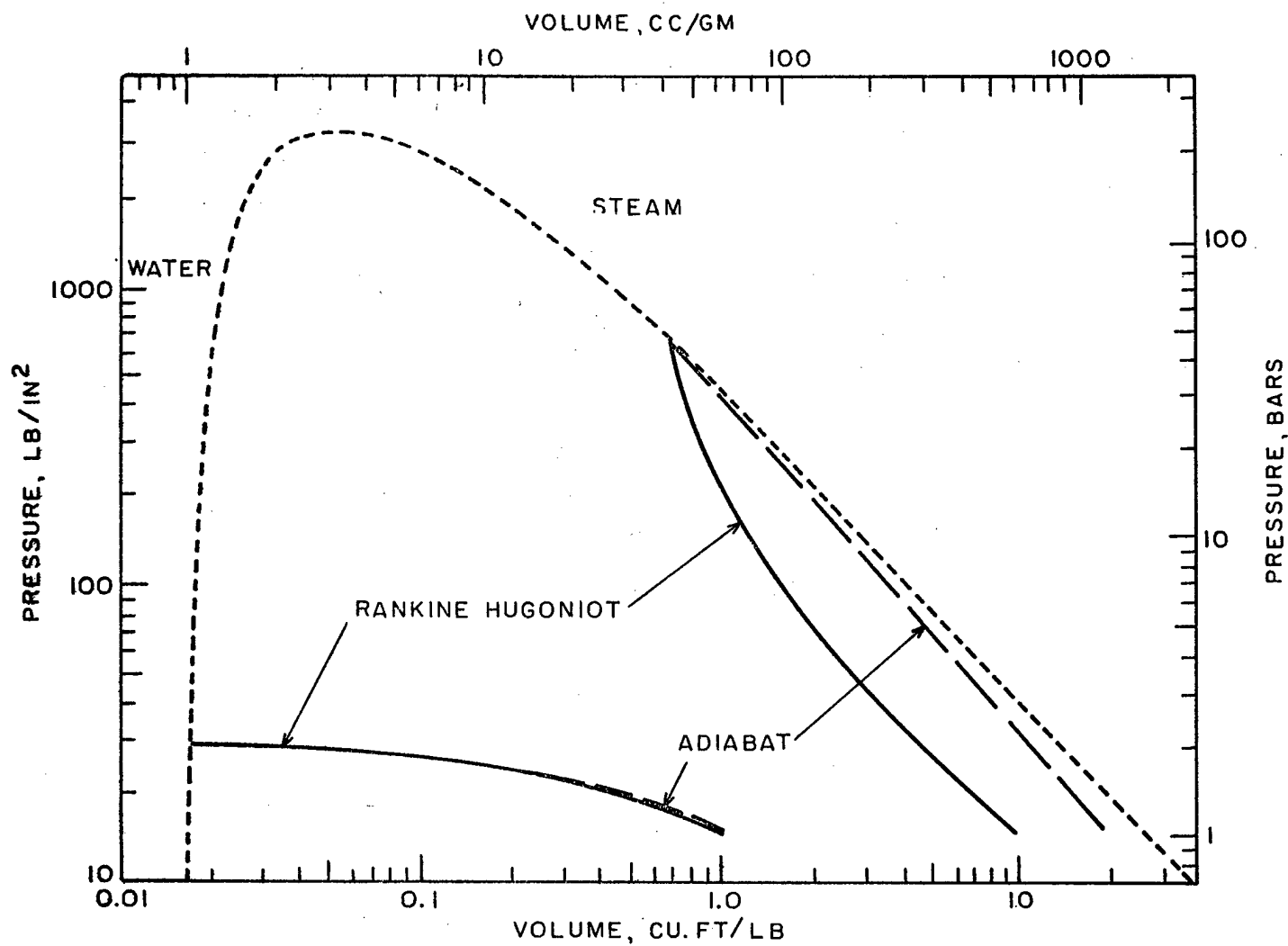ENTHALPY AT VARIOUS PRESSURES

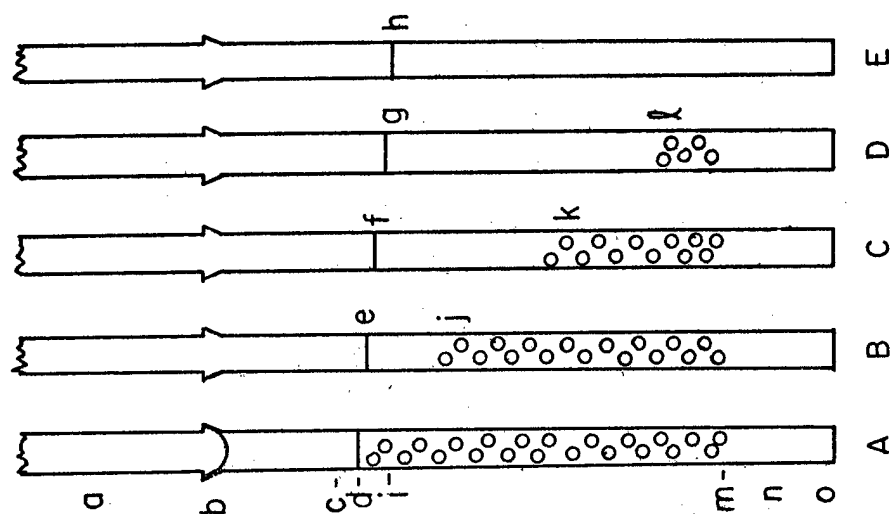Fig. 9 RANKINE-HUGONIOT CURVES AND ADIABATS IN A WATER-STEAM MIXTURE

Fig. 11 PRESSURE-TIME SEQUENCE AT POINTS c,i,j,k,o OF FIG. 10

Fig. 10 PICTORIAL REPRESENTATION OF "SHOCK" PROPAGATION THROUGH BOILING WATER

-45-
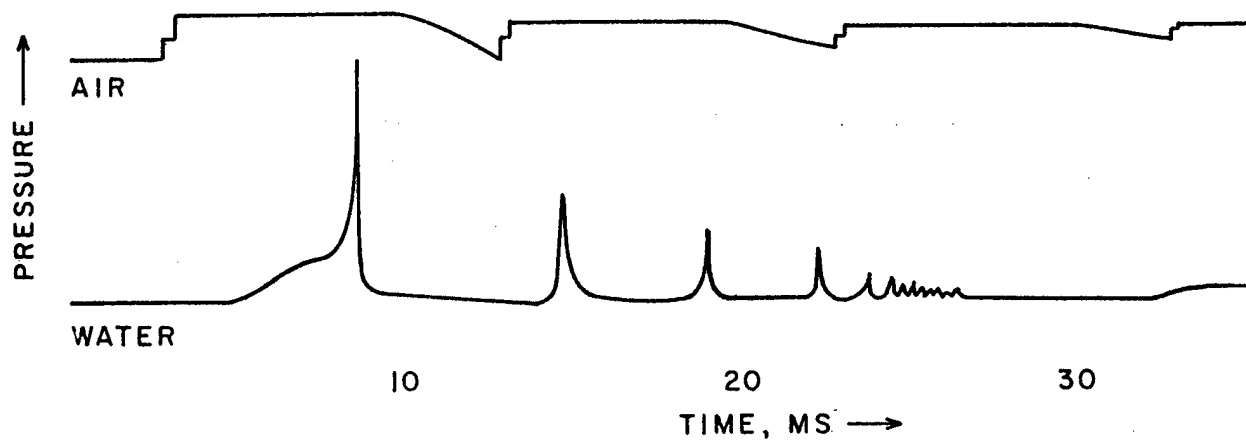
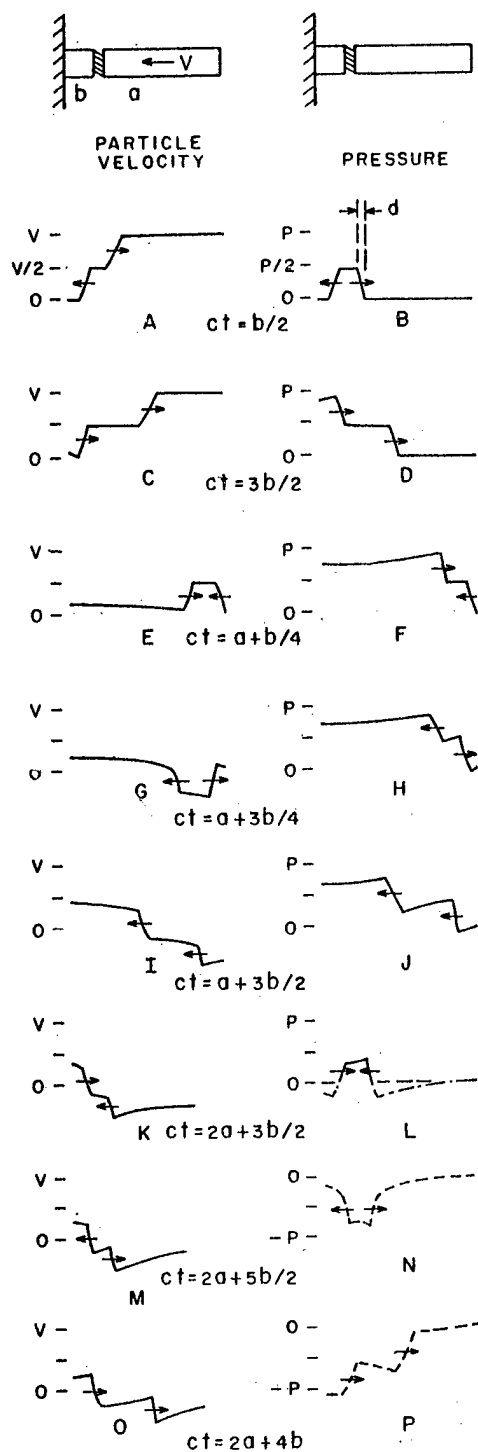Fig. 12 PRESSURE-TIME FUNCTION

Fig. 13 WATER HAMMER PULSE,
LONG MOVING COLUMN
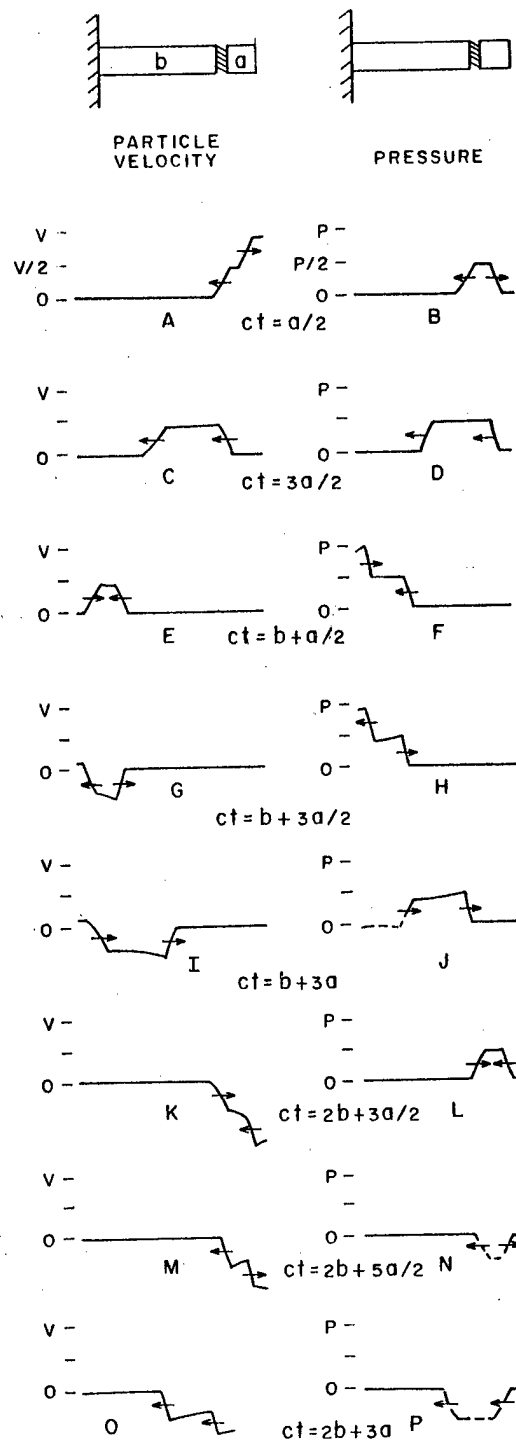
Fig. 14 WATER HAMMER PULSE,
SHORT MOVING COLUMN
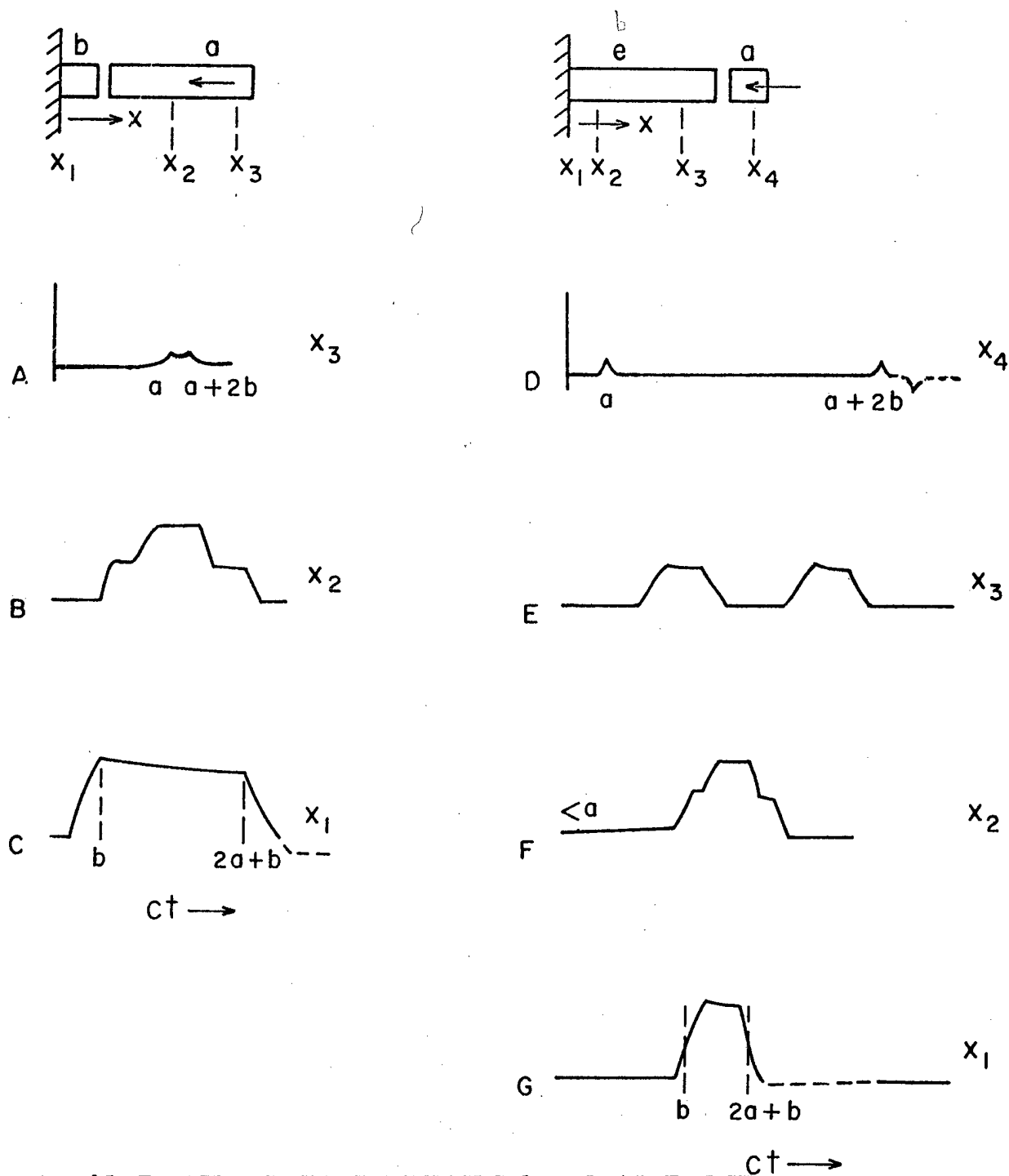
Fig. 15 PRESSURE-TIME DETAILS OF FINAL PULSE
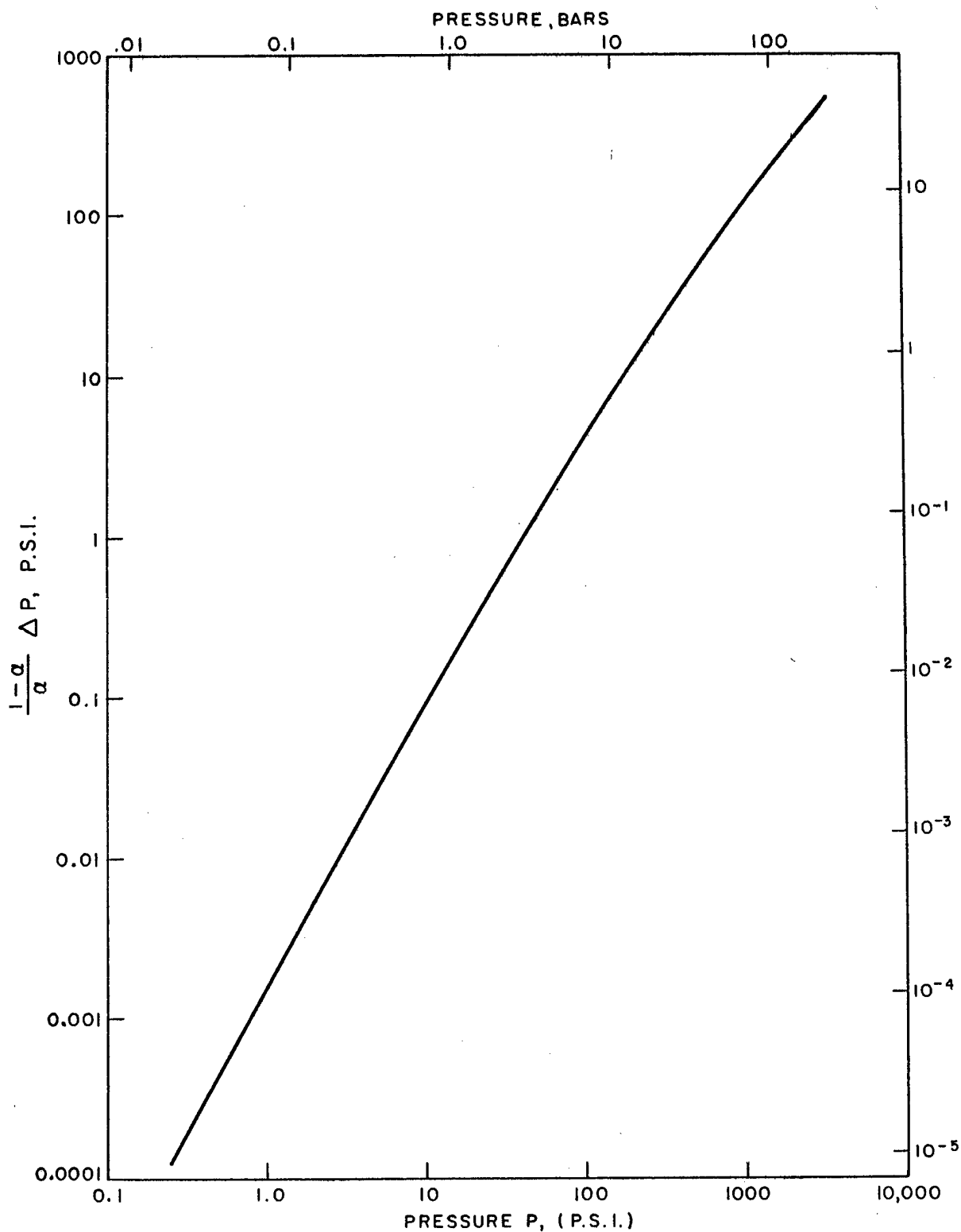
Fig. 16   MINIMUM PRESSURE OF PLANE PRESSURE FRONT
REQUIRED TO CONDENSE ALL THE STEAM
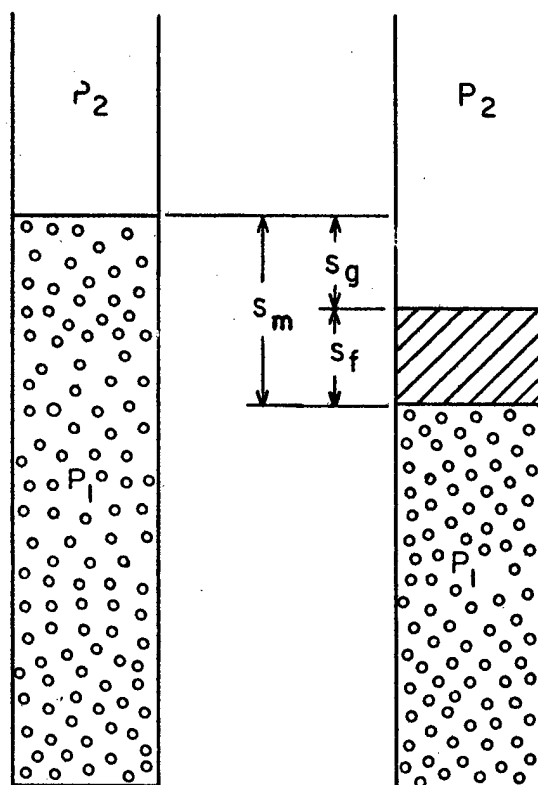
Fig. 17 PRESSURE PROPAGATION IN A BUBBLE MIXTURE

TO VACUUM

WATER

STEEL PIPE
1½ I.D.

DIAPHRAGM

TO PRESSURE

MANOMETER

GLASS PIPE

TO CATHODE
FOLLOWER

PRESSURE
GAUGE

HEATER
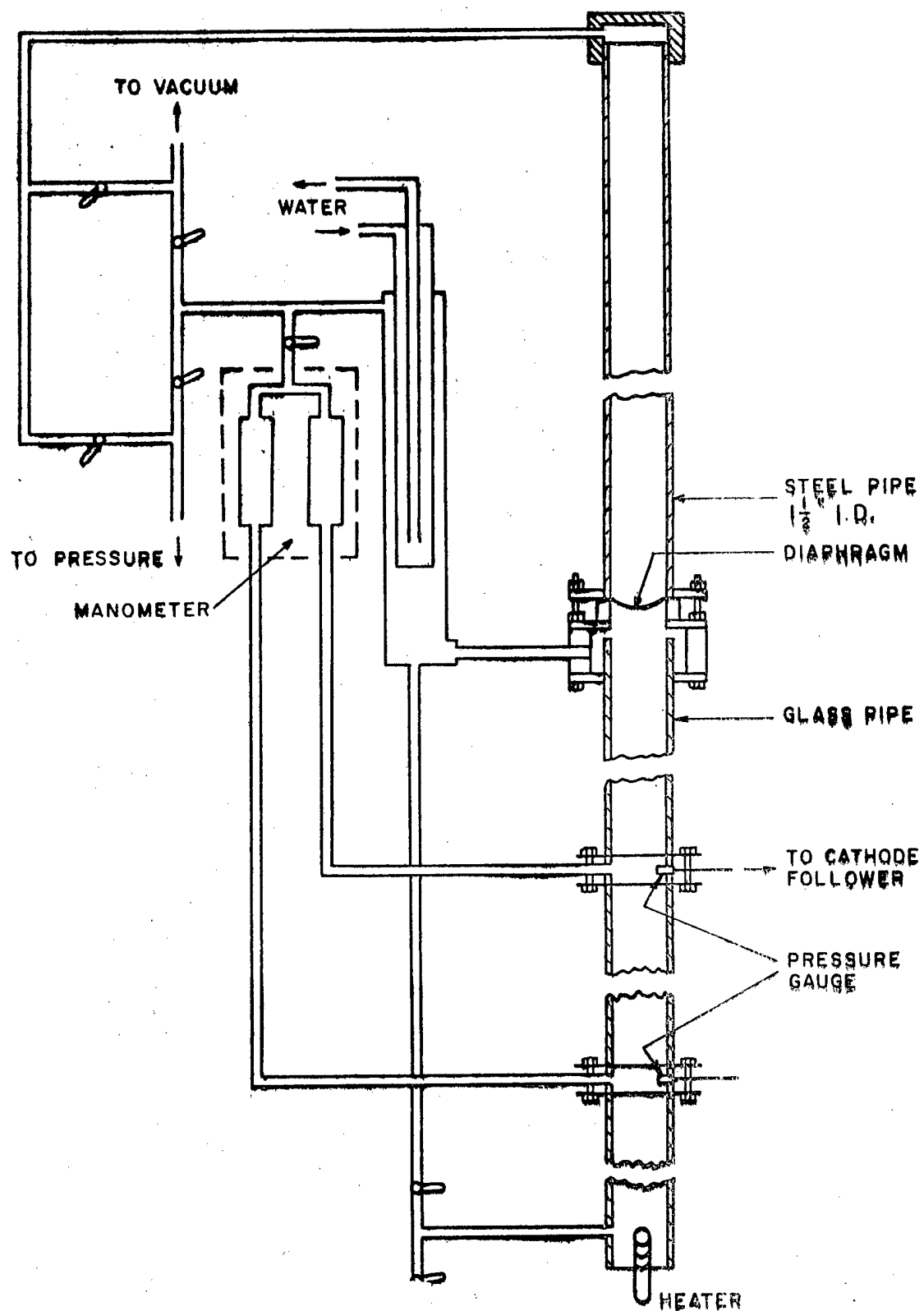
Fig. 18 DIAGRAM OF SHOCK TUBE
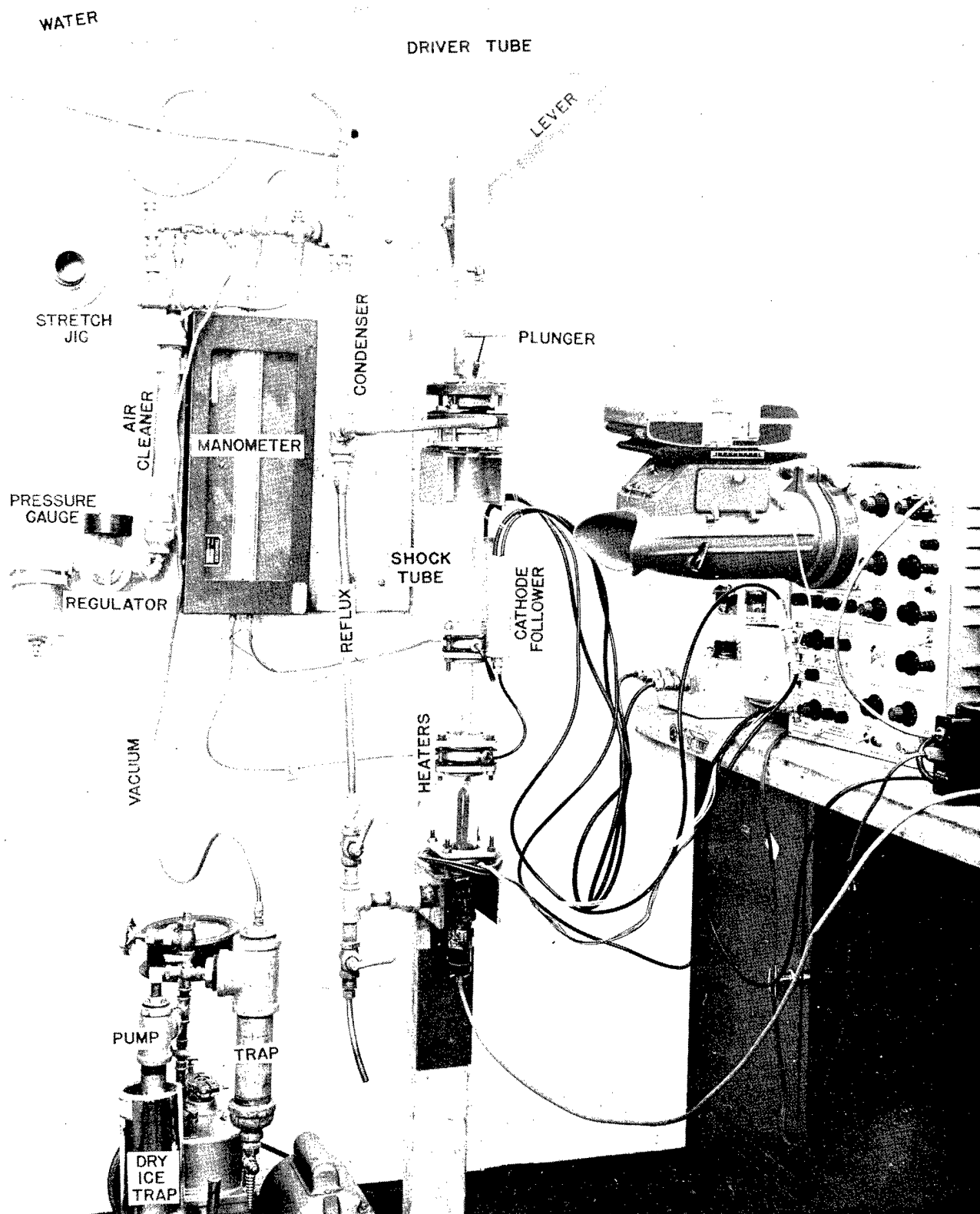
Fig. 19 VIEW OF APPARATUS
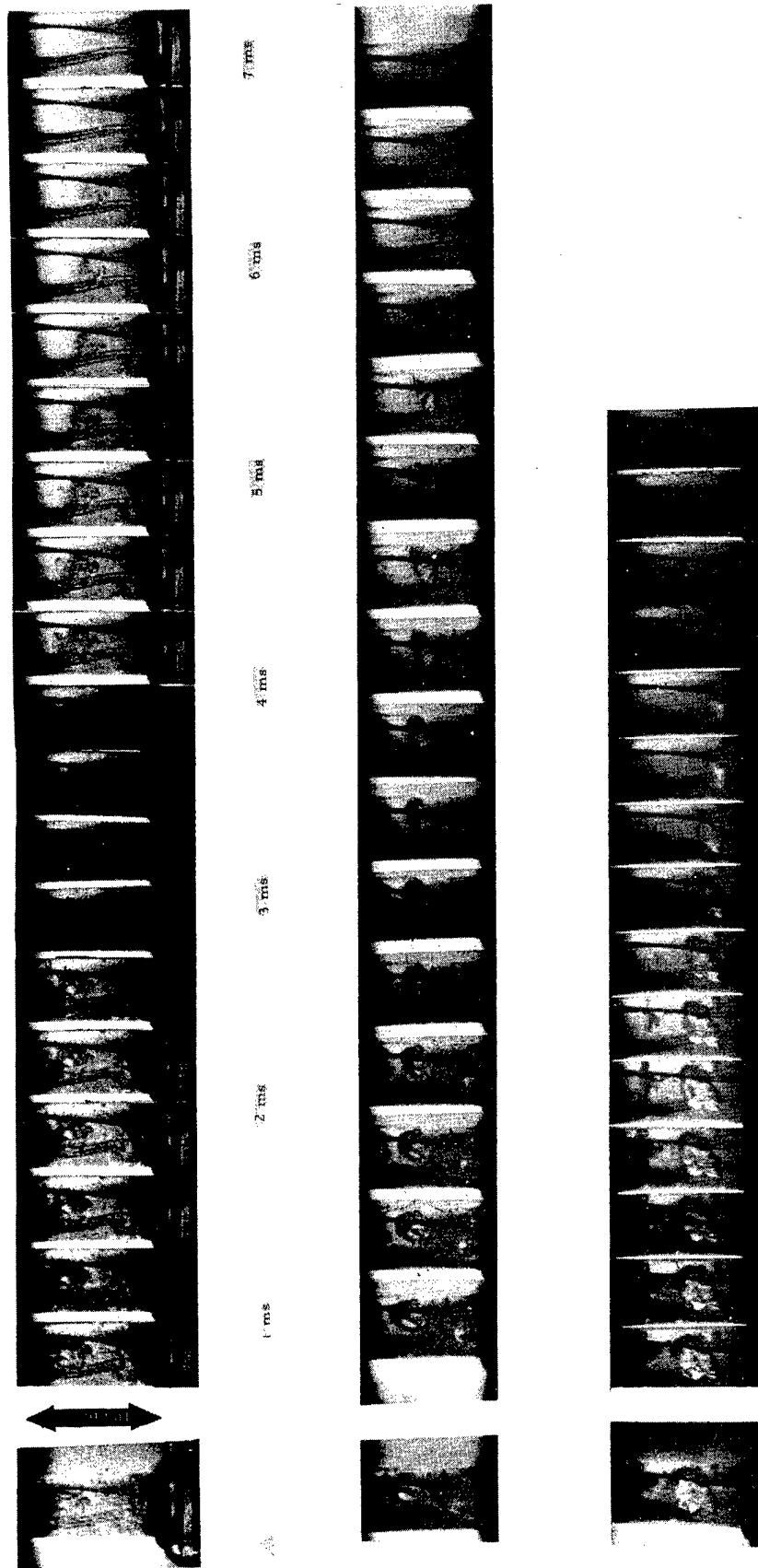
Fig. 20 PHOTOGRAPHIC TIME SEQUENCE OF STEAM BUBBLE COLLAPSE DURING A PRESSURE TRANSIENT

-53-
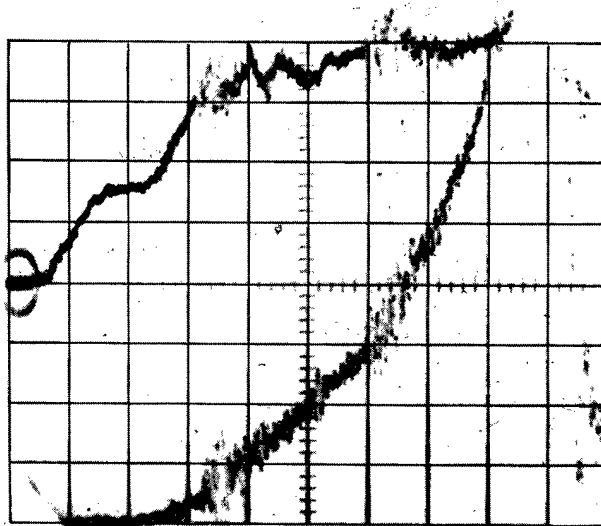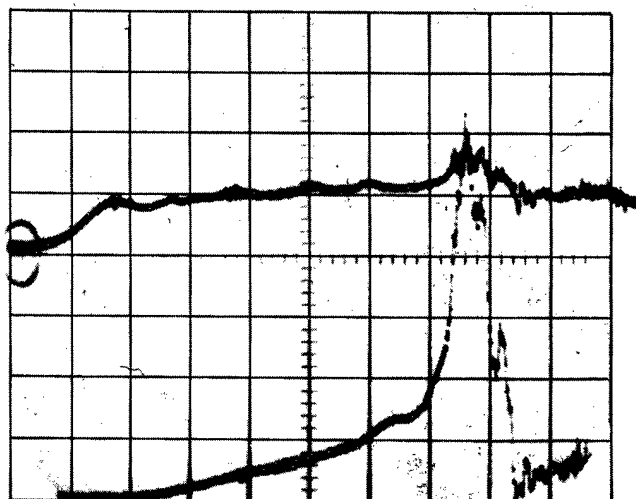
Fig. 21 VARIATION OF PRESSURE AT DISTANCES 1 cm AND 6 cm BELOW SURFACE; INITIAL BUBBLE CONCENTRATION, 5 PER CENT
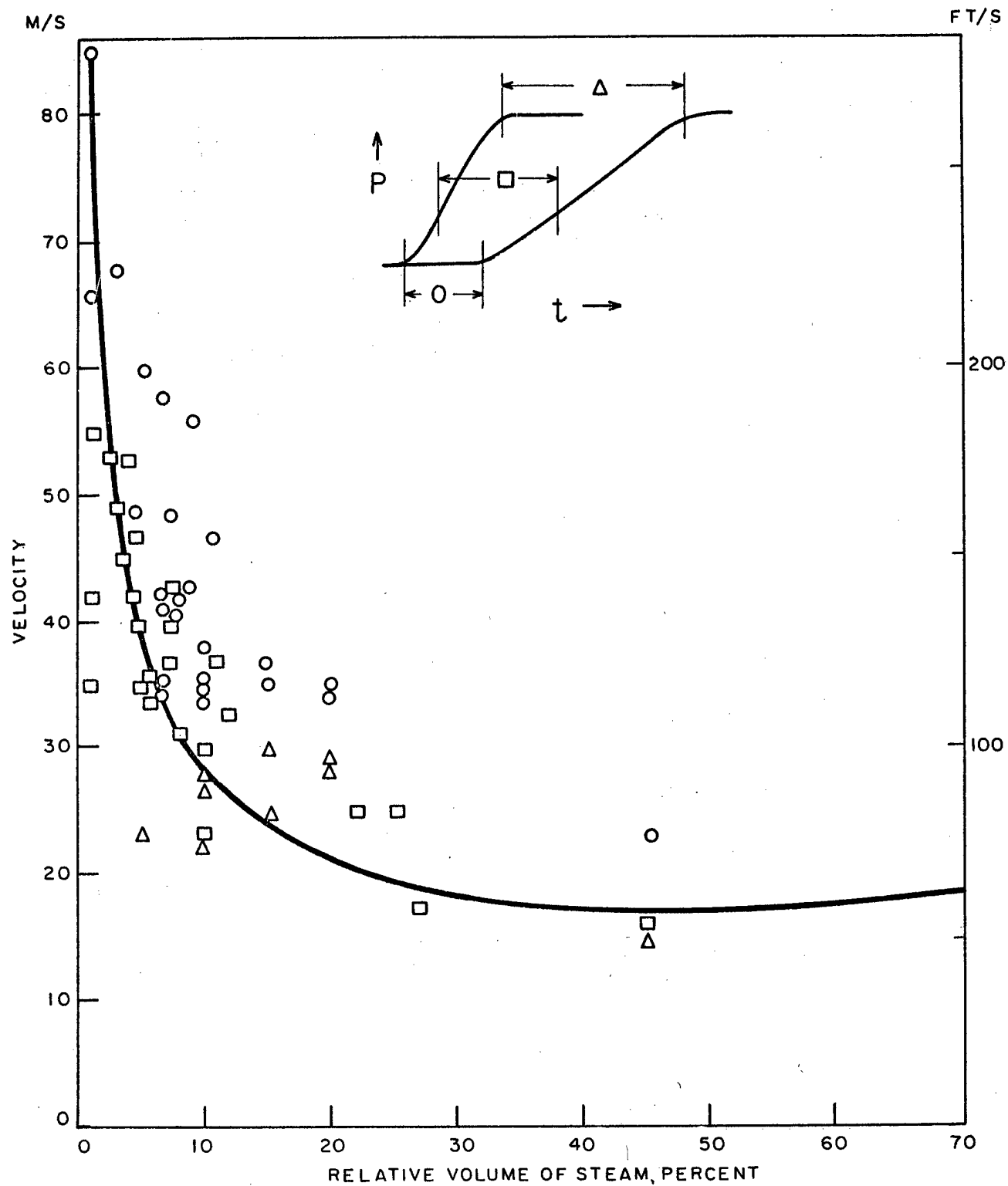
Fig. 22　VELOCITY OF PRESSURE WAVE IN BOILING WATER,
$p = .10$ psi (0.7 bars)

Report No.
ARF 4132-12
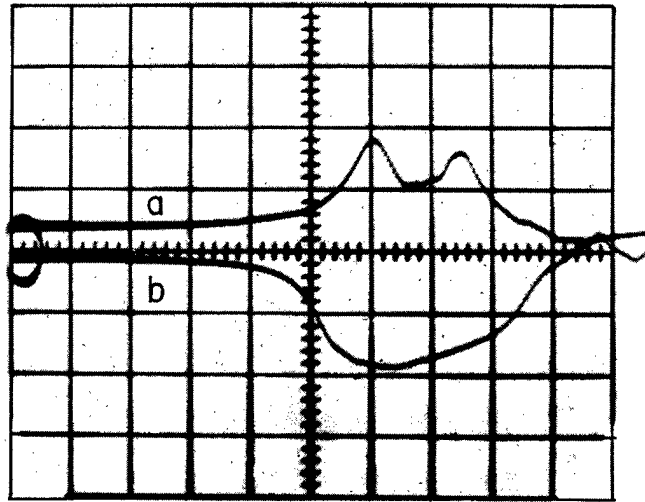
Fig. 23 ANALYSIS OF FINAL PULSE NEAR SURFACE (a)
AND AT LOWER END OF PIPE (b)
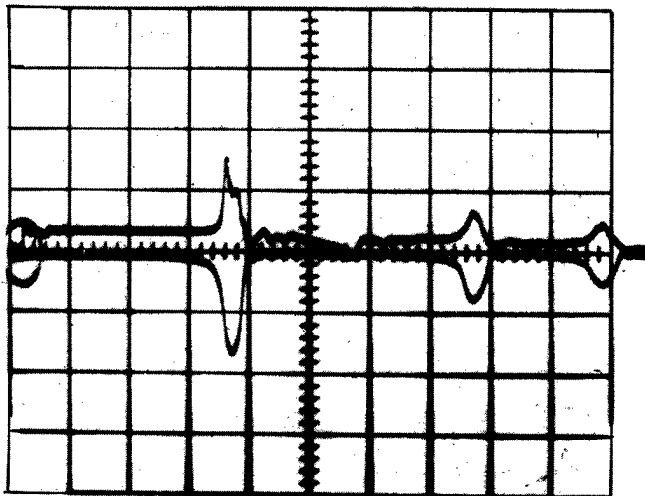
Fig. 24 SUCCESSION OF PULSES SHOWING LONG
INTERVALS DUE TO FORMATION BY
NEGATIVE PRESSURE

Fig. 25 STRETCHING THE DIAPHRAGM
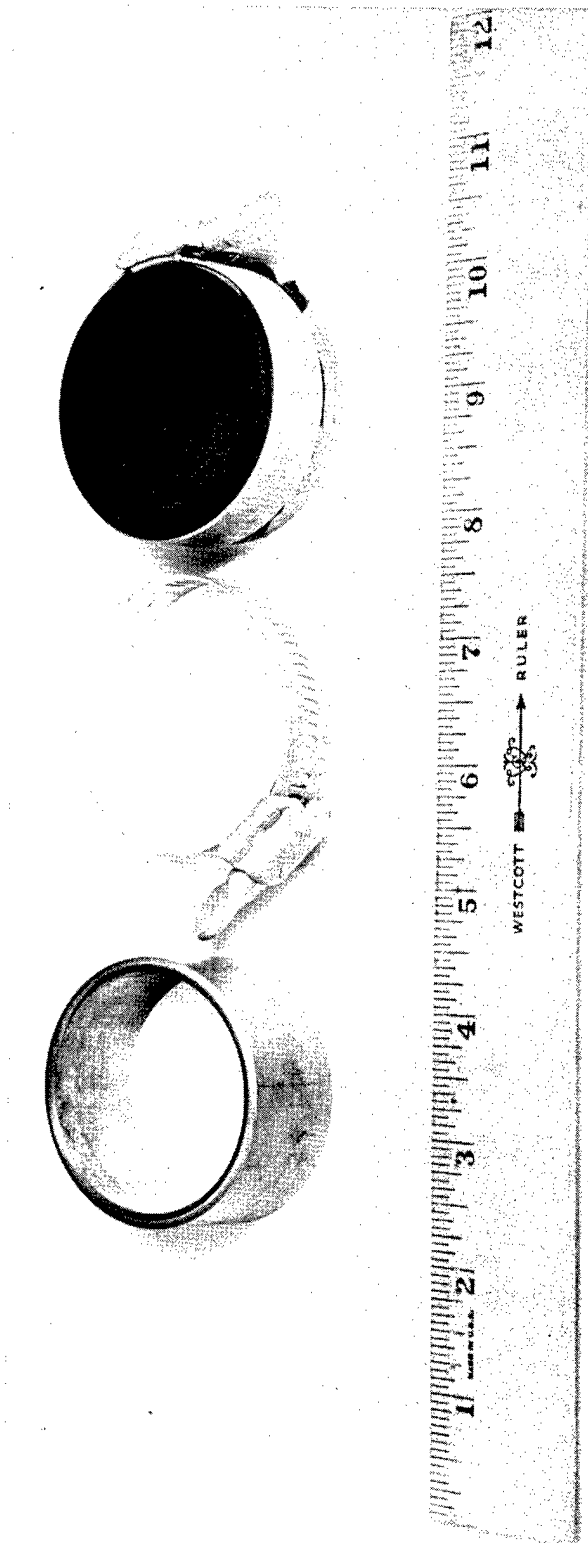
Fig. 26 DIAPHRAGM HOLDER

Report No.
ARF 4132-12

APPENDICES

APPENDIX A

DERIVATION OF THE VELOCITY OF SOUND IN A WATER-STEAM MIXTURE

Let

c = velocity of sound,

p = pressure,

ρ = density,

V = specific volume = $1/\rho$,

T = temperature,

S = entropy,

q = steam quality,

    = mass of steam/total mass.

Subscripts: f refers to the fluid (water)

          g refers to the gas (steam)

          e refers to the change of parameter on evaporation.

Thus $V_e = V_g - V_f$; $S_e = S_g - S_f$.

The basic equations are

$$c^2 = \left(\frac{\partial p}{\partial \rho}\right)_S = -V^2 / \left(\frac{\partial V}{\partial p}\right)_S , \tag{A-1}$$

$$dS = \left(\frac{\partial S}{\partial p}\right)_q dp + \left(\frac{\partial S}{\partial q}\right)_p dq , \tag{A-2}$$

$$dV = \left(\frac{\partial V}{\partial p}\right)_q dp + \left(\frac{\partial V}{\partial q}\right)_p dq , \tag{A-3}$$

$$S = q S_g + (1-q) S_f = q S_e + S_f , \tag{A-4}$$

$$V = q\,V_g + (1-q)\,V_f = q\,V_e + V_f\,. \qquad (A-5)$$

Since in (A-1) S = constant, dS = 0. Substituting this in (A-2) and rearranging,

$$dq = - \left[\left(\frac{\partial S}{\partial p}\right)_q \bigg/ \left(\frac{\partial S}{\partial q}\right)_p \right] dp\,. \qquad (A-6)$$
$$(dS=0)$$

Now differentiate (A-4) and (A-5), bearing in mind that V_e, V_f, a S_e, and S_f are not functions of q but are uniquely related to pressure:

$$\left(\frac{\partial S}{\partial q}\right)_p = S_e, \quad \text{and} \quad \left(\frac{\partial S}{\partial p}\right)_q = q\,\frac{dS_e}{dp} + \frac{dS_f}{dp}\ ; \qquad (A-7)$$

$$\left(\frac{\partial V}{\partial q}\right)_p = V_e, \quad \text{and} \quad \left(\frac{\partial V}{\partial p}\right)_q = q\,\frac{dV_e}{dp} + \frac{dV_f}{dp}\,. \qquad (A-8)$$

Substitute (A-4) and (A-7) in (A-6); then

$$dq = - (1/S_e) \left[q\,dS_e/dp + dS_f/dp \right]\ dp\,. \qquad (A-9)$$
$$(dS=0)$$

Substitute (A-8) and (A-9) in (A-3); then

$$dV = \left[q\,\frac{dV_e}{dp} + \frac{dV_f}{dp} - \frac{V_e}{S_e}\left(q\,\frac{dS_e}{dp} + \frac{dS_f}{dp}\right) \right]\ dp\,. \qquad (A-10)$$
$$(dS=0)$$

Collect the terms, so that

$$\left(\frac{\partial V}{\partial p}\right)_S = q\left(\frac{dV_e}{dp} - \frac{V_e}{S_e}\,\frac{dS_e}{dp}\right) + \frac{dV_f}{dp} - \frac{V_e}{S_e}\,\frac{dS_f}{dp}\ ; \qquad (A-11)$$

then

$$c^2 = \left(\frac{\partial p}{\partial \rho}\right)_S = \frac{V^2}{-(\partial V/\partial p)_S}\ ; \qquad (A-12)$$

that is

$$c = \cfrac{q\,V_e + V_f}{\left[-q\left(\cfrac{dV_e}{dp} - \cfrac{V_e}{S_e}\cfrac{dS_e}{dp}\right) + \cfrac{V_e}{S_e}\cfrac{dS_f}{dp} - \cfrac{dV_f}{dp}\right]^{1/2}} \; . \qquad\qquad (A-13)$$

This formula is correct for a self-consistent system of units.
The steam tables available give pressure in lb in.$^{-2}$, specific volume
in ft^3 lb^{-1}, and entropy in Btu per lb per °F. This system is not self-
consistent, and requires multiplication of the expression by $12\sqrt{g} = 68.099$
to convert inches to feet and pounds to slugs in order to give the velocity
in ft sec^{-1}.

One other parameter of interest is the impedance of the medium,
ρ c. Now

$$\rho = V^{-1} = (q\,V_e + V_f)^{-1}.$$

Hence

$$\rho c = \left[-q\,\frac{dV_e}{dp} + \frac{qV_e}{S_e}\frac{dS_e}{dp} + \frac{V_e}{S_e}\frac{dS_f}{dp} - \frac{dV_f}{dp}\right]^{-1/2} \; . \qquad\qquad (A-14)$$

For boiling water when $q < 10^{-3}$, this simplifies to

$$\rho c \cong \left[\frac{V_e}{S_e}\frac{dS_f}{dp} - \frac{dV_f}{dp}\right]^{-1/2} \; . \qquad\qquad (A-15)$$

This impedance has been tabulated in Table A-1.

Table A-1

IMPEDANCE OF BOILING WATER

p psi	Impedance		p bars
	$lb\ ft^{-2}\ sec^{-1}$	$gm\ cm^{-2}\ sec^{-1}$	
1	20.5	10.0	0.068
10	158	77.8	.68
20	294	142	1.36
50	625	308	3.4
100	1,050	517	6.8
200	1,960	965	13.6
500	4,070	2,000	34
1000	6,800	3,340	68
2000	11,400	5,610	136
3000	13,300	6,540	340
3206	~20,000	~10,000	364

We may simplify furthermore by considering that

$$\frac{dV_f}{dp} \ll \frac{V_e}{S_e} \frac{dS_f}{dp} \quad ; \tag{A-15}$$

then

$$(\rho c)^{-2} = \frac{V_e}{S_e} \frac{dS_f}{dp}$$

$$= (V_e/S_e)(dS_f/dT)(dT/dp)$$

$$= (V_e/S_e)(C_f/T)(V_e/S_e), \tag{A-16}$$

where we have defined the specific heat of the fluid $C_f = dQ/Dt =$ TdS_f/dT, and have made use of the Clausius-Clapeyron relation $dT/dp = V_e/S_e$. If we further define a latent heat $L = TS_e$, then

$$\rho c = S_e/(V_e \sqrt{C_f/T})$$

$$= L/(V_e \sqrt{TC_f}) . \tag{A-17}$$

The flow rate through a pipe is limited to the sonic velocity. The rate of mass flow of fluid under these so-called "choked" conditions is $A\rho c = AL/(V_e \sqrt{TC_f})$, where A is the area of the pipe.

APPENDIX B

USE OF STEAM TABLES TO COMPUTE THE VELOCITY OF SOUND

The quantities V_e, V_f, S_e and S_f required by the formula derived in Appendix A are found tabulated in Keenan and Keyes' steam tables[3]. The derivative of the quantities is obtained by a linear approximation from adjacent lines in the table, thus:

$$\left(\frac{dV_e}{dp}\right)_n \cong \frac{(V_e)_{n+a} - (V_e)_{n-b}}{p_{n+a} - p_{n-b}} \tag{B-1}$$

where p_n, etc., refer to the values in the nth lines of the table. In general, a and b were taken as unity; that is, values were computed from adjacent lines in the table except where the intervals were suddenly changed. In that case, a or b was chosen so that

$$p_{n+a} - p_n = p_n - p_{n-b} . \tag{B-2}$$

The error introduced by this technique is partly due to the fact that the slope of the chord differs slightly from the slope of the tangent at the mid-point of the arc, and partly due to the small differences between adjacent variables. Curve fitting with approximate analytical expressions and differentiating eliminates the first error, but not the second. That is, we cannot fit any curve any more accurately than the given points. The errors due to the difference between chord and tangent can be shown to be of the order of $(\Delta p/p)^2$ for the functions of interest (see Appendix C). Table B-1 gives a few values of $(\Delta p/p)^2$ and the percentage difference of the last digits of ΔV_e, ΔS_e, and ΔS_f. The precision of these last variables is the rounding-off in the last digit. In retrospect it appears

that the precision could have been increased somewhat by lengthening the chords, thus increasing the values of ΔV_e, ΔS_e, and ΔS_f and thereby decreasing the uncertainty in the last digit. This is especially true in the region of 100 psi. The optimum length of chord would be that for which the two errors here discussed are approximately equal. It was not considered worthwhile to repeat the calculations for this minor improvement of precision.

Table B-1

ERROR DUE TO CHORD APPROXIMATION

$\dfrac{p}{\text{lb in.}^{-2}}$	Δp	$\left(\dfrac{\Delta p}{p}\right)^2$ per cent	ΔV_e per cent	ΔS_e per cent	ΔS_f per cent
1	0.2	4.0	0.07	0.2	0.5
2	0.2	1.0	0.03	0.3	0.8
5	0.5	1.0	0.10	0.3	0.7
10	1.0	1.0	0.15	0.3	0.6
20	1.0	0.25	0.01	0.7	1.4
50	1.0	0.04	0.3	1.7	3.0
100	1.0	0.01	1.2	3.0	5.0
200	10.0	0.25	0.9	1.0	2.0
500	20.0	0.16	0.1	0.6	1.3
1000	100.0	1.00	0.1	0.2	0.3
2000	100.0	0.25	0.5	0.2	0.5

APPENDIX C

ERRORS INTRODUCED BY USING THE CHORD APPROXI-

MATION FROM STEAM TABLES

First consider the difference of slope between the chord and the tangent. The chord is chosen to be symmetrical about the point of interest as defined in Eq. (B-2). Over a limited region the value of V_e varies approximately as $1/\rho$ and S_e varies approximately as log p. For both these types of function we shall now show the error to be equal to $(\Delta p/p)^2$.

Case 1

$$y = x^n$$

$$y + \Delta y = (x + \Delta x)^n = x^n \left[1 + \frac{n\Delta x}{x} + \frac{n(n-1)}{1 \cdot 2} \left(\frac{\Delta x}{x}\right)^2 + - - \right] ,$$

$$y - \Delta y = (x - \Delta x)^n = x^n \left[1 - \frac{n\Delta x}{x} + - - \right] ,$$

$$2\Delta y = x^n \left[2\frac{n\Delta x}{x} + 2 \frac{n(n-1)(n-2)}{1 \cdot 2 \cdot 3} \left(\frac{\Delta x}{x}\right)^3 + - - \right] ,$$

$$\frac{\Delta y}{\Delta x} = nx^{n-1} \left[1 + \frac{(n-1)(n-2)}{2 \cdot 3} \left(\frac{\Delta x}{x}\right)^2 + - - \right] .$$

Now the definition of the tangent is the slope of the chord as $\Delta x \rightarrow 0$; thus $(1 + \frac{(n-1)(n-2)}{2 \cdot 3} \left(\frac{\Delta x}{x}\right)^2 +$ higher powers of $\frac{\Delta x}{x})$ is the error in using a chord symmetrically disposed about the point of interest. Now V_e varies approximately as p^{-1}. Hence, the chord symmetrically disposed about the point of contact differs from the tangent at that point by factor differing from unity by $(\frac{\Delta p}{p})^2$.

Case 2

$$y = \log x,$$

$$\Delta y = \log (x + \Delta x) - \log x,$$

$$\Delta y = \log (1 + \Delta x/x),$$

$$-\Delta y = \log (1 - \Delta x / x);$$

therefore

$$2\Delta y = \log (1 + \Delta x/x) - \log (1 - \Delta x / x)$$

$$= \Delta x / x + (\Delta x / x)^2 + (\Delta x / x)^3 + \text{---} + \Delta x / x - (\Delta x / x)^2 + (\Delta x / x)^3 + \text{---}$$

$$= 2 \Delta x / x + 2 (\Delta x / x)^3 + \text{---};$$

hence

$$\frac{\Delta y}{\Delta x} = \frac{1}{x} \left[1 + (\frac{\Delta x}{x})^2 + \text{---} \right].$$

Now S_e and S_f approximate a log p function over a limited regions, so here again chord errors are of the form $(\Delta p / p)^2$.

It should be noted that if a non-symmetrical chord is chosen to approximate the tangent, so that the one end of the chord is at a point of interest, then the error would have been $\Delta p / p$ instead of $(\Delta p / p)^2$. This is seen immediately in the above derivation, since the first terms in the binomial expansion cancel owing to the symmetrical disposition of the chord.

Report No.
ARF 4132-12

APPENDIX D

THE RELATIONSHIP BETWEEN VOLUME AND PRESSURE

ALONG A LINE OF CONSTANT ENTROPY

The expression for volume in terms of pressure (Section IV) may be obtained as follows:

As in Appendix A, we write

$$V = q\, V_e + V_f , \qquad\qquad q = (V - V_f)/V_e , \qquad\qquad \text{(D-1)}$$

$$S = q\, S_e + S_e , \qquad\qquad q = (S - S_f)/S_e ; \qquad\qquad \text{(D-2)}$$

thus

$$V = (S - S_f)\, V_e/S_e + V_f ,$$

$$= S\, V_e/S_e - (S_f\, V_e/S_e - V_f),$$

$$= S\, X_1 - X_2 . \qquad\qquad \text{(D-3)}$$

The parameters $V_e/S_e = X_1 (p)$ $\qquad\qquad$ (D-4)

and $S_f\, V_e/S_e - V_f = X_2 (p)$ $\qquad\qquad$ (D-5)

were plotted as a function of pressure.

Analytical expressions for X_2 are quite awkward, but by changing the arbitrary zero-reference for the specific entropy and calling this modified function X_3, simple power laws

$$X_1 (p) = Ap^{-a} + Bp^{-b}, \qquad\qquad \text{(D-6)}$$

$$X_3 (p) = Fp^{-f} , \qquad\qquad \text{(D-7)}$$

can be fitted to the functions

$$X_1 (p) = V_e/S_e ,$$

and

$$X_3 (p) = (V_e/S_e) (S_f + S_o) - V_f . \qquad\qquad \text{(D-8)}$$

Substituting Eq. (D-8) in (D-3), we obtain

$$V = (S + S_o) V_e/S_e - (S_f + S_o) V_e S_e - V_f$$

$$= (Ap^{-a} + Bp^{-b}) (S + S_o) - Fp^{-f}.$$

For the units in available tables, pressure in lb in.$^{-2}$ and specific volume in ft^3 lb^{-1}, the constants best fitting the curves were

A = 113,   B = 67.5,   F = 67.5 ,

a = 1,   b = 0.7,   f = 0.7,

S_o = 0.24.

The equality of B and F and of b and f then permitted further simplification to the final form,

$$V = A_o (S + S_o) p^{-1} + B_o (S + S_o - 1) p^{-0.7}, \tag{D-9}$$

Where $A = A_o$ and $B = B_o$. Numerical values of the constants in Eq. (D-9) are given in Table 2 for various systems of units.

APPENDIX E

MINIMUM PRESSURE NEEDED TO CONDENSE ALL THE STEAM

To obtain the minimum pressure needed to condense all the steam in a boiling mixture, we approach the problem from the other end by considering the small amplitude region and letting the pressure amplitude increase until we reach the point of complete condensation. In addition, we make use of the observation in Section II-C that the Rankine-Hugoniot in the boiling mixture is very close to the adiabat.

Next define the volume concentration of steam, α, and express it in terms of the mass concentration, q:

$$(1/\alpha - 1) V_g = (1/q - 1) V_f . \tag{E-1}$$

For boiling water $\alpha < 0.9$; mass concentration of steam, q, is very small so that we may write approximately

$$q \cong \alpha V_f / \left[(1 - \alpha) V_g \right], \tag{E-2}$$

and

$$d q/d\alpha \cong V_f / \left[(1 - \alpha)^2 V_g \right] . \tag{E-3}$$

Now for $q \ll 1$, Eq. (A-9) becomes

$$(\partial p/\partial q)_S \cong - S_e /(dS_f/dp). \tag{E-4}$$

Combining (E-3) and (E-4),

$$(\partial p/\partial \alpha)_S = - V_f S_e / \left[V_g (1 - \alpha)^2 (dS_f/dp) \right] . \tag{E-5}$$

To obtain the maximum pressure which just barely does not condense all the vapor, we integrate from the existing concentration α to zero and obtain:

$$P_{max} = - \int_{\alpha}^{0} (1 - \alpha)^{-2} V_f S_e \, d\alpha / \left[V_g (dS_f / dp) \right] \qquad (E-6)$$

$$= \alpha (1 - \alpha)^{-1} V_f S_e / \left[V_g (dS_f / dp) \right] . \qquad (E-7)$$

This is now of course also equal to the minimum "shock" pressure necessary to condense all vapor. Its value is plotted in Fig. E-1. Now let us substitute this minimum pressure into the Eq. (11a) to obtain the velocity of a pulse barely strong enough to condense all the vapor.

$$(u_1^2)_{min} = (p_2 - p_1)_{min} V_f / \left[\alpha (1 - \alpha) \right] \qquad (E-8)$$

$$= (1 - \alpha)^{-2} V_f^2 S_e / \left[V_g (dS_f / dp) \right] \qquad (E-9)$$

$$= V^2 S_e / \left[V_g (dS_f / dp) \right]. \qquad (E-10)$$

This is very similar in magnitude to the velocity of sound in the mixture, Eq. (A-13), using the following relations:

$$V = q V_e + V_f \cong V_f / (1 - \alpha),$$

and

$$q \, d V_e / dp - q (V_e / S_e)(dS_e / dp) + d V_f / dp \ll (V_e / S_e)(dS_f / dp) .$$

Thus the velocity of propagation of pulses of amplitude just sufficient to condense all the steam is approximately the sonic velocity.

Report No.
ARF 4132-12

APPENDIX F

PRESSURE MEASUREMENTS

The pressure was measured with quartz transducers (Kistler Instrument Company, Tonawanda, New York, Type 601). These gages have an overall diameter of 0.25 in. and an active diaphragm of about 0.12 in. The self-resonance frequency is 250,000 cps. A check with a shock wave in air traveling across the diaphragm showed that the time for the output to reach 90 per cent of its final value was less than 5 microseconds.

The gages were calibrated by two independent techniques. An electrometer calibrator, Kistler PZ-6, was used to measure the charge produced on the crystal for a static pressure produced by a dead weight tester.

An acoustic technique was also used. In this, the gage was subjected to a 1 kc alternating pressure produced by a loudspeaker in an air-filled cavity. The pressure was measured with a condenser microphone, for which a reciprocity calibration was available.

The pressure used in the first calibration was 500 psi; that used in the second was 0.15 psi. The sensitivity achieved with the former technique was about 10 per cent greater than that obtained with the latter. The precision of the latter technique is not expected to be better than that achieved; however, it provides a good check for the operation of the gage at audio frequency.

It was found convenient to connect the gages via cathode followers to the separate inputs of a switching amplifier (Tektronix Type 53/54C) to view the signals from the two stations separately. Special short cables (about 4 in.) were used, so that the load on the crystals was minimized (20 $\mu\mu$ f, 700 megohms). In this way the voltage sensitivity

(0. 1 v/cm) of the oscilloscope was adequate without further amplification.
An earlier scheme using the output of both gages on the same channel
worked well in a single phase medium (air), but led to unsatisfactory
pictures for pulses traveling through the mixture.

Report No.
ARF 4132-12

APPENDIX G

THE DIAPHRAGM

Some time had to be devoted to a search for a suitable diaphragm material, since standard plastic materials do not perform well at the temperature of boiling water. On the other hand operation at lower temperature and greatly reduced pressure proved to increase the difficulties in producing uniform mixtures. Tests with neoprene 0.015 in. thick and 0.031 in. thick were quite satisfactory. The material was stretched as far and as uniformly as possible, as shown in Fig. 25, on a ring slipped over a jig. A standard hose clamp held the material in place (Fig. 26). By the prestretching technique used, rapid opening of the diaphragm to well over three fourths of the ring area was assured. By making the ring 2 in. in diameter for use in conjunction with the 1-1/2 in. I. D. pipe, the remaining parts of the diaphragm presented no severe obstruction. A slight area change near the diaphragm was also required by the steam outlet. This, it was later shown, could have been greatly reduced. Small oscillations due to turbulence in this region were not very important because the time scale was so long that these turbulence-induced fluctuations were virtually completely damped out. A few observations of shock waves in air at a point 14 in. below the diaphragm indicated a well-formed shock wave at that point (rise time, as well as could be observed with available instruments, appeared to be less than 5 microseconds). The strength of the neoprene at elevated temperatures decreased with time, and if heated for a sufficiently long time, would sometimes burst without any applied air pressure. However,

for a few minutes the diaphragm would withstand over 75 per cent of its room-temperature bursting pressure (12 to 16 psi for the thin material, and 22 to 30 psi for the thicker one).

The use of neoprene rather than cellulose acetate or mylar as a diaphragm material has the advantage that the diaphragm ruptures cleanly and does not shatter, thereby maintaining the shock tube and valve system free of fragments and reducing the cleaning problem.

APPENDIX H

THE EQUILIBRIUM ASSUMPTION

The assumption of equilibrium conditions made at the outset of the analysis (Section II-A) is valid for sufficiently low frequencies and for particles of the discontinuous phase (that is, water droplets in steam, or steam bubbles in water) of sufficiently small size. From thermal diffusion we may estimate the frequency limit for particles of a given size, or the particle size limit for a given frequency, so that equilibrium conditions still hold.

Jakob and Hawkins: Elements of Heat Transfer[15] gives in Fig. IV-7 the temperature at the center of a sphere whose surface temperature is suddenly raised. This curve plots $(T_{ct} - T_s)/(T_{co} - T_s)$, the ratio of the difference between the center temperature T_{ct} at time t and the surface temperature T_s, to the initial difference in temperature $(T_{co} - T_s)$ at time t = 0, when the surface temperature was raised from T_{co} to T_s. A few points taken from this graph have been tabulated in Table H-1 in terms of the dimensionless quantity $4\alpha t/D^2$ where α is the thermal diffusivity of the sphere and D is its diameter.

Table H-1

CENTER TEMPERATURE OF A SPHERE

$4\alpha t/D^2$	0.1	0.15	0.2	0.3	0.4	0.5
$\dfrac{T_{ct} - T_s}{T_{co} - T_s}$	0.7	0.4	0.25	0.1	0.04	0.01

From this table we see that most of the heat transfer has taken place in a time such that $4\,\alpha t/D^2$ has values between 0.1 and 0.5. Without going into the details of the temperature distribution throughout the sphere at each instant and calculating the heat fluxes, we see that a very large fraction of the total heat transfer has taken place when $4\,\alpha t/D^2$ has the value 0.2. From this we obtain a time constant $t = .05\,D^2/\alpha$ in which we may say all heat transfer has taken place. The reciprocal of this time constant will give us the value of the frequency below which the equilibrium assumption is satisfactory. This frequency has been tabulated in Table H-2 for liquid drops in vapor and vapor bubbles in liquid.

Table H-2

FREQUENCY LIMIT FOR EQUILIBRIUM ASSUMPTION

Frequency Limit For	Diameter, mm:	1.0	0.1	0.01
		Frequency, cps		
water at 32°		2.8	280	28,000
water at 400°		3.4	340	34,000
saturated vapor at 32°		31,000	3.1×10^6	3.1×10^8
saturated vapor at 200°		340	3.4×10^4	3.4×10^6
saturated vapor at 400°		25	2.5×10^3	2.5×10^5
saturated vapor at 600°		5.5	5.5×10^2	5.5×10^4